CHALMERS

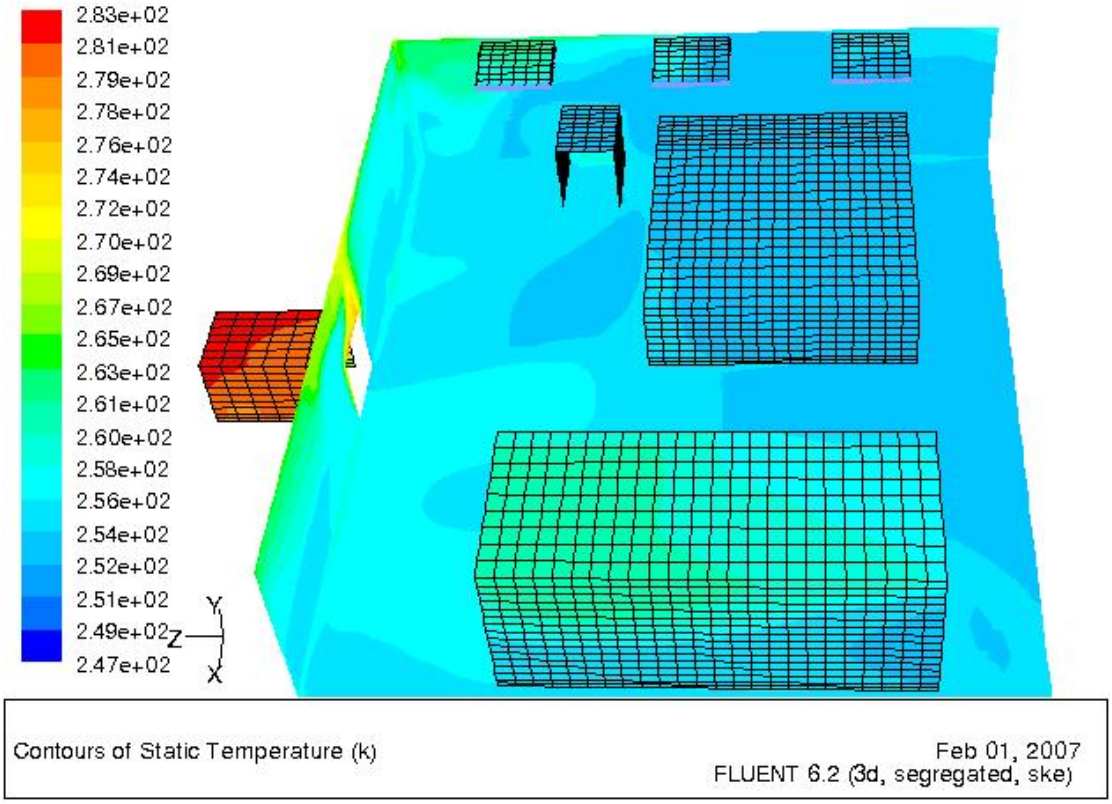

Computational Modeling of Temperature Distribution in a Freeze Room

BJÖRN MARGEIRSSON

Course: TME050 - Project Course
Department of Applied Mechanics
Division of Fluid Dynamics
CHALMERS UNIVERSITY OF TECHNOLOGY
Gothenburg, Sweden, 2007

Abstract

One of the largest fishing industry companies in Iceland, HB Grandi, operates a freeze room for fish at Norðurgarður in Reykjavík. The freeze room has two doors which can have serious effects on the overall temperature distribution in the freeze room if opened for a long time. In this work air flow and temperature distribution in the freeze room is modeled in 3D with the CFD software FLUENT. The aspects that are investigated include the influence of wind velocity outside the building and possible addition of an open hall outside one of the doors. Both steady and unsteady computations are carried out. Validation by comparison with measurements is limited because of quite many uncertainties concerning the measurements.

Keywords: CFD, FLUENT, steady, unsteady, temperature distribution, freeze room

Acknowledgements

I would like to thank the financial sponsor of this project; MATÍS – Food research, Innovation & Safety in Iceland. Special thanks for practical suggestions go to Sigurjón Arason at MATÍS and Sigurður Gunnarsson at HB Grandi. Last but not least, I would like to thank my supervisor at Chalmers, Dr. Håkan Nilsson, for his theoretical guidance and suggestions concerning the calculations.

Nomenclature

Roman Symbols

A	Area [m^2]
c_p	Heat capacity [J/kg/K]
d	Diameter, height [m]
h	Convective coefficient [$W/m^2/K$]
k	Thermal conductivity [W/m/K]
L	Length [m]
Nu	Nusselt number [-]
Pr	Prandtl number [-]
p	Pressure [Pa]
q	Heat rate [W]
q_w	Heat rate from a wall [W]
$\vec{q}''$	Heat flux [W/m^2]
R	R value; thermal resistance per area [m^2K/W]
R_{th}	Thermal resistance [K/W]
Re	Reynolds number [-]
T	Temperature [K, °C]
T_f	Film temperature [K, °C]
T_s , T_w	Wall temperature [K, °C]
T_∞	Free stream temperature [K, °C]
U	Overall heat transfer coefficient [$W/m^2/K$]
V	Wind velocity [m/s]

Greek Symbols

Δx	Wall (section) thickness [m]
ρ	Density [kg/m^3]
v	Kinematic viscosity [m^2/s]

Super- and Subscripts

exp, EXP	Experimental
CFD	Calculated; Computational Fluid Dynamics
f	Film (temperature) [K, °C]
p	Pressure [Pa]

Contents

1 Introduction

HB Grandi is a leading company in the Icelandic fishing industry with over 300 employees. The company lays great emphasis on keeping up with the technical evolution for fishing and processing that has been going on in the world. Large effort is put in keeping the quality of the product, the caught fish, in optimal levels all the way from it is caught until it is in the hands of the consumer. An important step on the way is the freezing process that takes place in one of the company's freeze room which is located at Norðurgarður in Reykjavik. In this freeze room as much as 18 thousand tons of packed pollock and redfish are annually refrigerated and kept frozen until time has come to be transferred to an exporting ship. In order to optimize the quality of the product it is important that the fore mentioned refrigeration process takes as short time as possible. Therefore should the temperature in the freeze room preferably never exceed -24 °C, especially at the location in the room where the fish pallets are placed.

A layout of the room and its surroundings can be seen in Figure 1 below. The freeze room has two doors which can have serious effects on the temperature distribution in the room when opened. The west door is opened when fresh and newly packed fish is transferred into the freeze room from a packing room west of the freeze room. The south door, on the other hand, is opened when the frozen fish is to be moved out from the room to a ship. Because of possible wind outside the freeze room (and thereby forced convection instead of natural convection) opening of the south door is more critical for the temperature raise in the freeze room than opening of the west door. Therefore is the present study limited to opening of the south door.

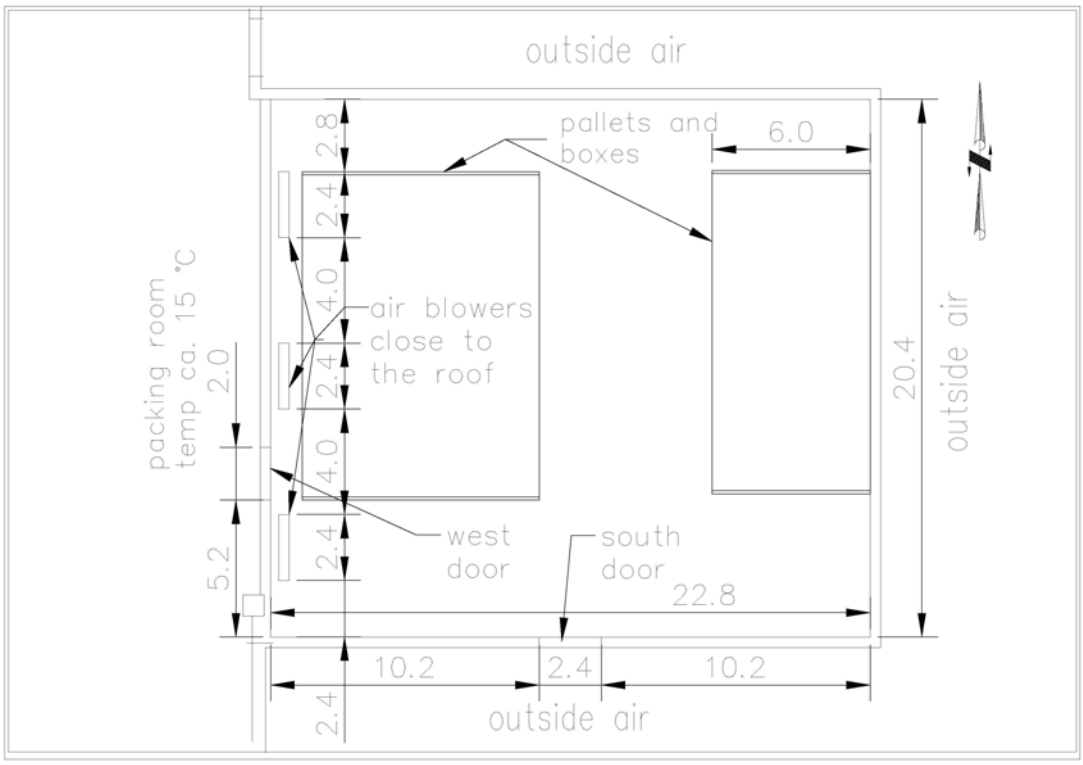

Figure 1. Outlay of the freezing room. All dimensions are in meters

The main objective of this work is to investigate numerically the influence of southerly wind blowing through open south door on the temperature distribution in the freeze room. In addition, existence of a hall which might be added to the building outside the south door in order to decrease the convective heat transfer through the door.

The grid generation software GAMBIT was used for grid design and the model developed was investigated using the Computational Fluid Dynamics (CFD) code FLUENT. To validate the model, predicted temperature values were compared with measurements that were done on the temperature distribution in the freeze room in 2004 [6].

Flick and Moureh [2] used FLUENT to perform a numerical simulation for a refrigerated truck and in the present study recommendations from their work are followed. Other CFD codes that have been used to study similar cases include PHOENICS [16] and CFX [7].

2 Theory

2.1 Heat Transfer

Heat transfer can be viewed as thermal energy in transit due to a temperature difference. Heat transfer can occur in three modes, i.e. conduction, convection and radiation. Since this study is limited to conduction and convection this chapter also excludes the radiation. The interested reader about radiation may wish to consult [8] and [13] for some theory of radiation.

Some theory of how to estimate the convection coefficient is given in chapter 3.4 instead of presenting it in this chapter.

2.2 Conduction Heat Transfer

When a temperature gradient exists in a medium, thermal energy is transferred due to random translational, rotational and vibrational motions of particles. The direction of the energy transfer is from the high temperature region to the low temperature region. The quantity of energy transferred (heat flux) per unit time and per unit area perpendicular to the direction of transfer is given by Fourier's law [13]:

$$\vec{q}''=-k\nabla T=-k(\vec{i}\,\frac{\partial T}{\partial x}+\vec{j}\,\frac{\partial T}{\partial y}+\vec{k}\,\frac{\partial T}{\partial z}) \quad \textbf{(1)}$$

where k is the thermal conductivity of the medium, T is temperature, $\frac{\partial T}{\partial x}$, $\frac{\partial T}{\partial y}$ and $\frac{\partial T}{\partial z}$ are the x, y and z components of the temperature gradient. The minus sign is inserted to satisfy the second principle of thermodynamics, i.e. heat flow is downhill the temperature scale. The heat rate is a product of the heat flux and the area perpendicular to the heat transfer:

$$\vec{q}=\vec{q}''\bullet A \quad \textbf{(2)}$$

The one dimensional heat rate through a homogeneous wall (in the x-direction) is given by:

$$q=-kA\frac{\partial T}{\partial x} \quad \textbf{(3)}$$

2.3 Convection Heat Transfer

Convection can be defined as transfer of thermal energy both due to conduction and advection [13]. When fluid moves past a surface with different temperature a thermal boundary layer is developed. At the surface (wall) and very close to it the only physical mechanism of convective heat transfer is a conduction process. Newton's law of cooling is used to express the overall effect of convection:

$$q=hA(T_s-T_\infty) \quad \textbf{(4)}$$

where h is the convection heat transfer coefficient, T_s is the wall temperature and T_∞ is the undisturbed temperature of the surrounding fluid.

Convection is natural or free if no external source of motion is found, i.e. when the movement of air is experienced as a result of density gradients close to the surface. Common values for the convection coefficient (h) in natural convection are

between 2 and 10 W/m^2/K, depending on the temperature difference and geometry of the subject.

Forced convection is on the other hand generated by external means and the convection coefficient is a lot higher than for the natural convection. Combined convection is a combination of the free and forced convection types.

2.4 Thermal resistance, R Values and Overall Heat Transfer Coefficient

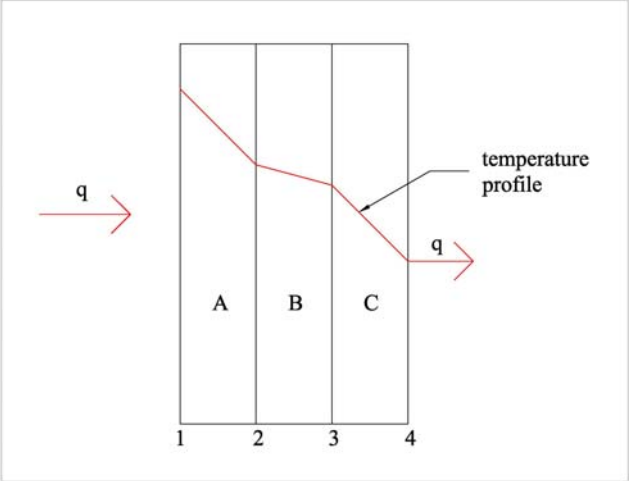

Figure 2. One dimensional heat transfer through a composite wall

According to [8], integration of equation **(3)** yields for a multi layer wall, like can be seen in Figure 2:

$$q = -\frac{k_A A}{\Delta x_A}(T_2 - T_1) = -\frac{k_B A}{\Delta x_B}(T_3 - T_2) = -\frac{k_C A}{\Delta x_C}(T_4 - T_3) \quad \textbf{(5)}$$

It should be noted that the heat flow must be the same through all sections. T_1, T_2, T_3 and T_4 are the temperatures of the wall section faces and Δx is the wall section thickness. Solving equations **(5)** simultaneously the heat flow can be written as:

$$q = \frac{T_4 - T_1}{\frac{\Delta x_A}{k_A A} + \frac{\Delta x_B}{k_B A} + \frac{\Delta x_C}{k_C A}} \quad \textbf{(6)}$$

The heat rate may be considered as a flow, and the combination of thermal conductivity, thickness of material and area as a resistance to this flow. The temperature is the driving function for the heat flow and the Fourier's law can be written as:

$$q = \frac{\Delta T_{overall}}{\sum R_{th}} \quad \textbf{(7)}$$

where $R_{th} = \frac{\Delta x}{kA}$ are the thermal resistances of the various materials of the wall sections.

Insulating materials have lower thermal conductivity than others. In the building industry it is a common practice to use the term R value for classifying the performance of insulation. The R value is defined as:

$$R=\frac{\Delta T}{q/A} \tag{8}$$

The R value has the unit [K m^2/W] and the relation between it and the thermal resistance is simply

$$R=R_{th}\bullet A\,. \tag{9}$$

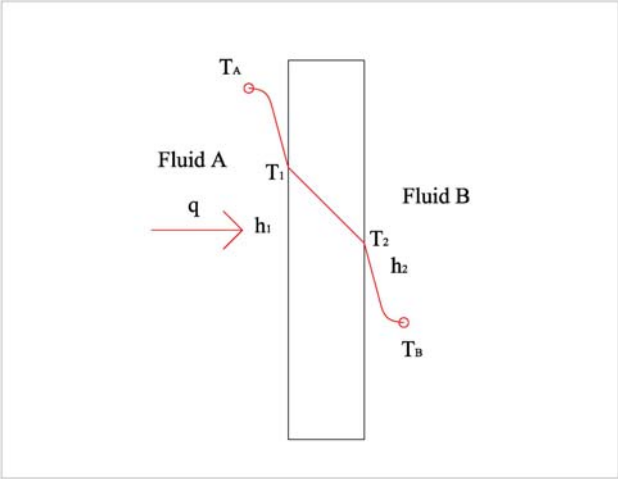

Figure 3. Overall heat transfer through a plane wall

Figure 3 above shows a plane wall with two surrounding fluids of different temperatures. The heat transfer can be expressed by

$$q=h_1A(T_A-T_1)=\frac{kA}{\Delta x}(T_1-T_2)=h_2A(T_2-T_B) \tag{10}$$

Solving these equations simultaneously like for equations **(5)** before, the heat flow can be written as

$$q=\frac{T_A-T_B}{1/h_1A+\Delta x/kA+1/h_2A} \tag{11}$$

Here the convective resistance is represented by 1/hA and the conductive resistance by Δx/kA. An overall heat transfer coefficient is frequently used to express the overall heat transfer by combined conduction and convection. This overall heat transfer, U, is defined by the following relation:

$$q=UA\Delta T_{overall} \tag{12}$$

When equations **(11)** and **(12)** are compared the overall heat transfer coefficient is yielded as

$$U=\frac{1}{1/h_1+\Delta x/k+1/h_2} \tag{13}$$

Finally, the overall heat transfer coefficient can be related to the R value in equation **(8)** through

$$U=1/R \tag{14}$$

3 Numerical Modeling

3.1 Solver

The segregated solver is used with the PISO pressure-velocity coupling scheme. According to [3] PISO coupling is recommended for all time dependent flow calculations, especially if a large time step is used. Since a second order discretization scheme normally yields less numerical diffusion than a first order scheme and since the second order discretization scheme for momentum did not result in an unstable solution it was used. The Boussinesq model was adopted and according to advice in [3] a Body Forced Weighted method was used as the discretization method for pressure. The principal objective in using the QUICK scheme for energy is to reduce the grid size required to yield a grid-independent solution, compared to the lower-order schemes. Turbulence is not emphasized and therefore only first order scheme is used when solving for it.

It was only necessary to use lower under-relaxation factors than the default ones in FLUENT in the first few iterations in the steady cases. The default values could be used through the whole unsteady calculations.

In the unsteady cases a first order implicit formulation was used since it is sufficient for most problems (see [3]). A fixed time stepping method was used with a time step of 0.5 seconds and according to residual plots, convergence was reached within the maximum limit of 10 iterations per time step.

3.2 Computational Domain

A layout of the computational domain is presented in Figure 4. In order to examine the influence of a southerly wind of different strength a 10 m long volume was added south of the building. Such a large domain outside the building proved necessary because adopting a lot smaller domain resulted in unrealistic solution for the velocity outside the building using the boundary conditions described in Chapter 3.4. The inside height of the freeze room is 5.5 m and the part of the computational domain south of the building reaches 5 m above the roof as can be noted in the figures of the grids in Chapter 3.5.

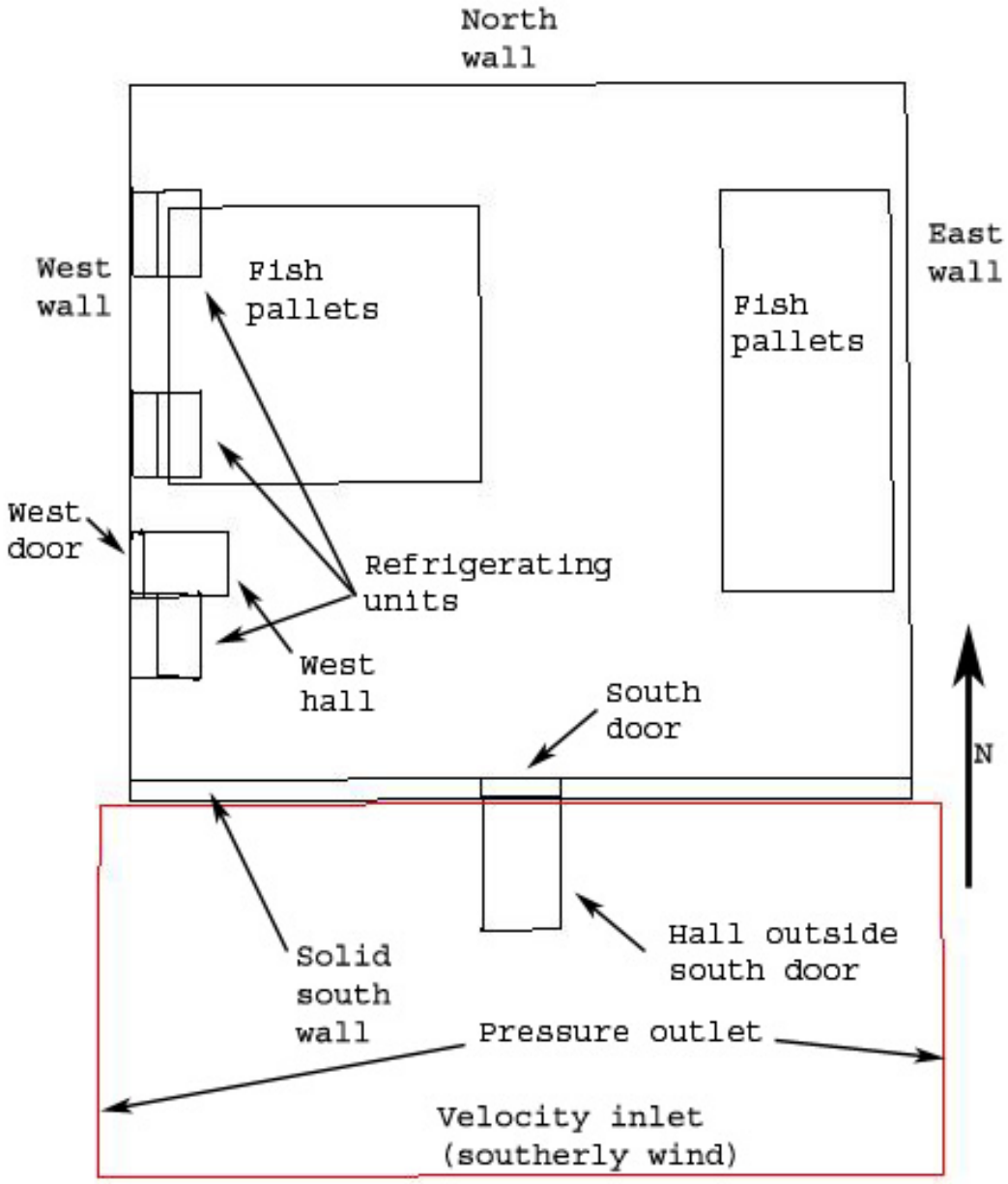

Figure 4. Layout of the computational domain including a hall in front of the south door

3.3 Cases

Sixteen different cases were studied and they are compared in Table 1. Cases 1 – 4 are run in order to investigate grid dependency; how coarse mesh could be used in the rest of the calculations without yielding significantly different solutions for different grids. The standard case assumed wind velocity of 10 m/s from south but in cases 5, 6, 8, 9, 11, 13 and 15 different wind velocity values were adopted in order to investigate the influence of wind velocity on the temperature distribution in the freeze room. This was done for both the two kinds of steady cases (open and closed south door) and even for the time dependent (unsteady) cases.

The solution from the corresponding steady case with closed door was used as an initial solution for the unsteady cases 14 – 16. Finally, in order to examine the effects of having a 4 m long hall south of the south door case 16 was run with the solution from the corresponding case 12 as an initial solution. The maximum time length of the time dependent cases was 4 minutes.

Table 1. Overview of the cases

Case nr.	Time dependency	Grid	Flow (wind) velocity at inlet [m/s]	South door open/closed	Includes a hall in front of south wall
1	steady	G1	10	open	no
2	steady	G2	10	open	no
3	steady	G3	10	open	no
4	steady	G4	10	open	no
5	steady	G1	0	open	no
6	steady	G1	15	open	no
7	steady	G1	10	closed	no
8	steady	G1	0	closed	no
9	steady	G1	15	closed	no
10	steady	G5	10	open	yes
11	steady	G5	15	open	yes
12	steady	G5	10	closed	yes
13	steady	G5	15	closed	yes
14	unsteady	G1	10	closed in the beginning, then opened	no
15	unsteady	G1	15	closed in the beginning, then opened	no
16	unsteady	G5	10	closed in the beginning, then opened	yes

3.4 Boundary Conditions

3.4.1 Refrigeration Units

The number of refrigeration units is three and they are located close to the top of the 5.5 m high freezing room (see Figure 5). Each unit roughly consists of three air blowers, an evaporator and an air duct. The blower sucks the air from behind of the unit and blows it across an evaporator which removes heat from the air so it cools down before it flows out of the openings of the rectangular ducts. The openings are divided into three parts each with the approximate dimensions 40 x 80 cm (height x width).

Figure 5. Refrigeration unit seen from below situated in the south-east corner of the freezing room

Velocity inlet boundary condition is used for the duct openings. Based on the fact that the free flow height of some of the openings is reduced by aluminum plates (see Figure 6) an average opening height is estimated as 12 cm and adopted for all openings.

Figure 6. Duct opening in the middle refrigeration unit showing an aluminum plate inside the duct

The flow velocity out of the ducts was measured and the average value of 8.0 m/s is used as an inlet boundary condition along with the average measured temperature, -26 °C. The back side of the refrigeration units (see Figure 7) is modeled as a negative velocity inlet with temperature -24 °C and the velocity set so the mass flux through these outlets is the same as through the openings of the ducts described above. No information about the blowers is in place and the flow in the refrigeration units themselves is not investigated.

Figure 7. Back side of a refrigeration unit showing the three blowers which blow the air across the evaporator

3.4.2 Heat Conduction through Walls and Doors

The most important factor in the heat transfer into and out of closed buildings is normally the heat conductivity of the materials in the walls, roof and floor. In order to decrease the heat transfer through walls they are insulated with some insulated material(s) with very low conductivity compared to the building material. Based on the fact that considerably high temperature difference is demanded between the inside of the plant and the surroundings big emphasis is placed on the insulation. All walls are therefore insulated with 40 cm thick layer of styrofoam (extruded polystyrene). It has heat conductivity of 0.033 W/m/K compared to 1.75 W/m/K for concrete, which is 20 cm thick in all walls. The values used for heat capacity are 0.88 kJ/kg/K and 1.3 kJ/kg/K for concrete and styrofoam respectively. In order to simplify the problem the walls are considered homogenous with the R value (defined as the thermal resistance per area) calculated as

$$R_{wall} = R_{conc.} + R_{st.foam} = \left(\frac{\Delta x}{k}\right)_{conc.} + \left(\frac{\Delta x}{k}\right)_{st.foam} = \frac{0.2}{1.75} + \frac{0.4}{0.033} = 0.114 + 12.121 = 12.24 \text{ m}^2\text{K/W}$$

And since the total wall thickness is $\Delta x_{wall}=0.6$ m this R value corresponds to a heat conductivity of $k_{wall}=\Delta x_{wall}/R_{wall}=0.6/12.24=0.049$ W/m/K . These values for wall thickness and conduction coefficient are used for all walls except the floor. The weighted mean heat capacity for the wall is 1.16 kJ/kg/K and the weighted mean density is 833 kg/m^3 (adopting the density values of 2400 kg/m^3 for concrete and 50 kg/m^3 for styrofoam).

The floor is insulated with "only" 20 cm of styrofoam and using the same concrete thickness as before (20 cm) results in wall thickness of 0.4 m, an R value of 6.18 m^{2}K/W, a conduction coefficient of 0.065 W/m^2/K, weighted mean heat capacity of 1.09 kJ/kg/K and weighted mean density of 1225 kg/m^3.

The doors consist basically of 15 cm thick styrofoam base layered completely with aluminum of thickness 5 mm. The weighted mean heat capacity for the doors is 1273 kJ/kg/K and the weighted mean density is 217 kg/m^3 (using the density values of 871 kg/m^3 for aluminum and 50 kg/m^3 for styrofoam). Using the same method as before to calculate the conductivity for the 16 cm thick doors results in a heat conductivity of 0.035 W/m^2/K but a value of 0.05 W/m^2/K is adopted in order to cover possible leakage of air between the doors and the walls.

3.4.3 Heat Convection outside Walls and Overall Heat Transfer

The heat convection between the outside air and the walls of the freezing plant is estimated by using few different correlations for heat convection. Since southerly wind is dominant in Reykjavik during the summertime a common value of 10 m/s southerly wind is assumed when the heat convection coefficient is evaluated.

East Wall and Roof

To estimate the convection coefficient (h) for the east wall and the roof some well known correlations for flow parallel to a flat plate are considered. One of the most common correlations for the average Nusselt number is presented by Holman [8] as

$$\overline{Nu_L} = \frac{\bar{h}L}{k} = (0.037 Re_L^{0.8} - 871) Pr^{1/3} \qquad \textbf{(15)}$$

which gives the average convection coefficient for the whole length of the plate as

$$\bar{h}=\frac{k}{L}(0.037Re_L^{0.8}-871)Pr^{1/3} \quad \textbf{(16)}$$

This equation applies for turbulent flow with $5 \times 10^5 < Re_L < 10^7$ and uniform T_w and takes into account the laminar region at the beginning of the plate. For Re_L between 10^7 and 10^9 Holman suggests the following equation:

$$\overline{Nu_L}=\frac{\bar{h}L}{k}=[0.228Re_L(\log Re_L)^{-2.584}-871]Pr^{1/3} \quad \textbf{(17)}$$

Properties are evaluated at the film temperature, defined as the arithmetic mean between the wall and the free stream temperature:

$$T_f=\frac{T_w+T_\infty}{2} \quad \textbf{(18)}$$

The following similar equation is suggested by Lienhard [11] to calculate $\bar{h}$:

$$\overline{Nu_L}=\frac{\bar{h}L}{k}=0.0370Re_L^{0.8}Pr^{0.43} \quad \textbf{(19)}$$

This equation may be used for both uniform T_w and uniform q_w and Re_L up to about 3×10^7. It ignores the laminar region at the front of the plate. The equations above come from turbulent boundary layer theory and Sartori [14] compares them to empirical equations used for flat plate solar collectors. One of the equations that Sartori referred to is presented by Watmuff, Charters and Proctor [17]:

$$\bar{h}=2.8+3.8V \quad \textbf{(20)}$$

where V is the wind velocity. Lunde [12] suggests the following similar correlation, also referenced by Sartori:

$$\bar{h}=4.5+2.9V \quad \textbf{(21)}$$

Yet another equation having a similar form as equations **(20)** and **(21)** is proposed by Sharples and Charlesworth [15]:

$$\bar{h}=9.4V^{0.5} \quad \textbf{(22)}$$

Interesting is the fact that none of the three equations **(20)**, **(21)** or **(22)** take the length of the plate into account. On the other hand, equations **(15)**, **(17)** and **(19)** are dependent on the length through the Reynolds number. Comparison is shown between the different correlations and wind velocities and the results presented in Table 1. The Reynolds number for V = 10 m/s is calculated as $Re = VL/\nu = 10 \times 20.4 / 1.39 \times 10^{-5} = 1.5 \times 10^7$ so equation **(16)** does not apply in this case.

Table 2. Comparison of $\bar{h}$ [W/m^2/K] values from Nusselt relations and empirical correlations.

V [m/s]	Eq. **(15)**	Eq. **(17)**	Eq. **(19)**	Eq. **(20)**	Eq. **(21)**	Eq. **(22)**
10	-	21.3	20.9	32.8	33.5	29.7

Good agreement is reached between the equations from boundary layer theory (Eq. **(17)** and **(19)**) while the more simple equations **(20)**, **(21)** and **(22)** give noticeably

larger values for the average convection coefficient. In Sartori's paper it is noted that the Nusselt relations from boundary layer theory include the decay of the heat transfer that exists along the length of the surface. Because of this Sartori states that these equations tend to calculate more accurately the convection coefficient and therefore the results from Eq. **(17)** and **(19)** are used in the present work. The convection coefficient 21 W/m^2/K is adopted for both the east wall and the roof.

South and North Walls

The southerly wind, that is assumed, blows perpendicular to the south and north walls of the building. Thus other relations than for the east wall and the roof must be used in order to estimate the convection coefficient for the south and north walls. The present case may be compared to air flow cross a rectangular cylinder which has been studied by e.g. Igarashi [9]. According to Igarashi the overall Nusselt number may be calculated as

$$\mathrm{Nu}=\frac{hd}{k_f}=0.095\mathrm{Re}_{df}^{\,2/3} \qquad \textbf{(23)}$$

where

$$\mathrm{Re}_{df}=\frac{Vd}{\nu_f} \qquad \textbf{(24)}$$

Because of the ground the building is seen as half of a rectangular cylinder so d (the height of the cylinder) notes the double height of the walls which is 5.5 m. This gives h= 8.4 W/m^2/K. However, it must be mentioned that the present case deviates from Igarashi's because in his experiment the axial length normal to the flow was 15 times larger than the height compared to only around 2 times larger in the present case (length of south wall / double height of south wall = 22.8/10 = 2.28). This short length of the south and north walls should though only matter at the east side since the southerly wind is hindered from flowing west of the plant. It should also be noted that the Reynolds numbers in the present work are not within the limits of Igarashi's correlations and that the free stream temperature in his experiments was around 20 °C. Using similar relation presented by Holman [8]:

$$\mathrm{Nu}_{df}=\frac{hd}{k_f}=0.102\mathrm{Re}_{df}^{\,0.675}\mathrm{Pr}_f^{\,1/3} \qquad \textbf{(25)}$$

gives higher but comparable coefficient; 9.2 W/m^2/K. However, equation **(25)** applies only for 5 x 10^3 < Re_{df} < 10^5 and in the present study V = 10 m/s corresponds to Re_{df} = 7.9 x 10^6 so Eq. **(25)** is hardly applicable.

It can be learned from Igarashi [10] that the heat transfer coefficient for both the front side (south wall in the present case) and also the back side (north wall) of a rectangular cylinder is considerably larger than for the top of it (roof). Based on this fact and how hardly Eq. **(23)** and **(25)** are usable for the present case the heat transfer for the south wall is roughly estimated as 30 % larger than for the roof or 27 W/m^2/K. Judging by [11] the difference is not as big for the back side so the coefficient for the north wall is roughly estimated as 20 % larger than for the roof or as 25 W/m^2/K.

West Wall

The convective heat transfer outside the west wall differs from the other walls because west of the plant there is a packing room with indoor air (temperature around 17 °C). Thus no wind is found there and the convection is natural or free but not forced as along the other walls. Natural convection can normally be neglected compared to forced convection and therefore it was roughly estimated with a simple relation [8]:

$$h=1.31(\Delta T)^{1/3} \quad \textbf{(26)}$$

where ΔT is the difference between the temperature at the wall and far away from the wall in the packing room. If this temperature difference is 1 °C then h = 1.3 W/m^2/K and the h-value corresponding to 10 °C is 2.8 W/m^2/K. This shows that the convective coefficient is definitely small compared to at the other walls and value of 2 W/m^2/K chosen to estimate it.

Overall Heat Transfer Coefficient

It has previously been found that the R value for conduction through the wall is 12.24 m^{2}K/W. This value should be compared to the overall R value through and outside the walls (with convection included) which may be calculated as

$$R_{\text{overall}} = R_{conduction,wall} + R_{convection,outside\_wall} = 12.24 + 1/h \quad \textbf{(27)}$$

The estimated values for h result in an overall R value between 12.27 and 12.74 m^{2}K/W. This small difference between the overall resistance and the conduction resistance indicates that the more important heat transfer mechanism is by far conduction, i.e. convection outside the plant is not important. However, since already estimated the values for h were adopted as a convection boundary condition on the outside of the walls. Since the gravel below the floor prevents convection to occur there the overall R-value for the floor is just the same as the conduction R-value (6.18 m^{2}K/W).

It should be noted that in the cases with no wind and with the wind speed as 15 m/s the same values for the convection coefficients outside the walls were used. This should not affect the results much since the conduction is the dominant factor as has already been mentioned.

3.4.4 Fish Pallets

The model included two solid blocks of fish which represent the various quantities of frozen fish that can be found in the freeze room. The metric dimensions of the two blocks are 5 x 11.9 x 4.8 and 9.5 x 8.5 x 2.5 and the thermodynamic properties adopted for the fish are the following:

- heat conductivity: k_{fish} = 1.22 W/m/K (see [4])
- heat capacity: $c_{p\text{-}fish}$ = 2100 J/kg/K (see [1])
- density: ρ_{fish} = 1050 kg/m^3 (see [1])

3.4.5 Pressure Outlets

The sides and the top of the computational domain outside the building are defined as pressure outlets with the static gauge pressure of 0 Pa, backflow turbulence intensity of 3 % and backflow hydraulic diameter according the same as the hydraulic diameter of each side.

3.4.6 Wind Inlet

A velocity inlet was used for the wind inlet which was found 10 m south of the south wall. The turbulence intensity was defined as 5 % and the hydraulic diameter as 60 m.

3.5 Grids

The grids were all completely structured, made of hexagonal cells in the whole domain. The coarsest grid, G1, was sparingly made of 78 912 cells and the three finer grids used for studying grid dependency consisted of 117 488, 235 512 and 367 250 cells, respectively. Grid G5, which included the south hall, was just as coarse as G1 but the additional hall resulted in 82 282 cells compared to 78 912 for G1.

Grid G5 is shown in Figure 8 and comparison between G5 and G3 is presented in Figure 9 and Figure 10.

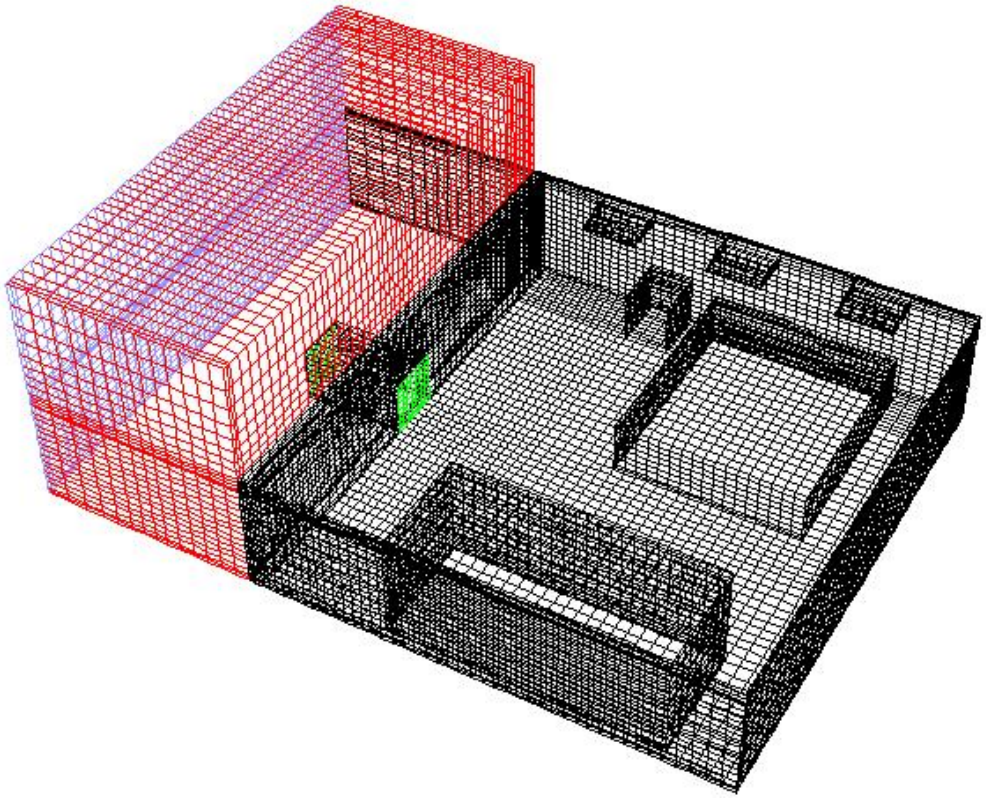

Figure 8. Grid G5. The walls of the freeze room are black, the red color represent a pressure outlet boundary condition, the blue color a velocity inlet and the green color an interior face (the open south door in this case)

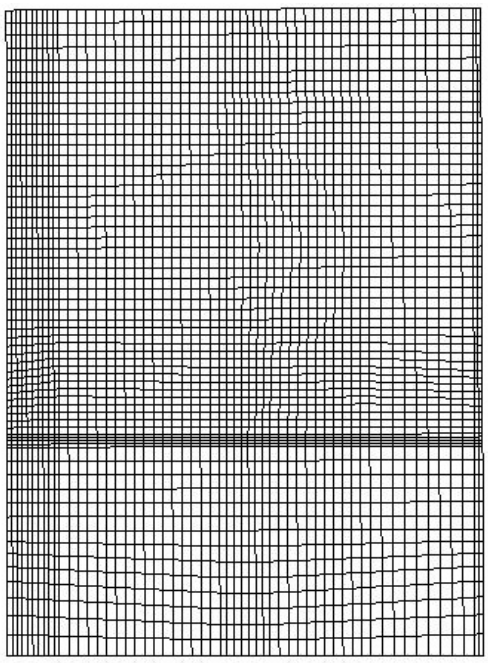

Figure 9. Grid G5 1.5 m above the floor

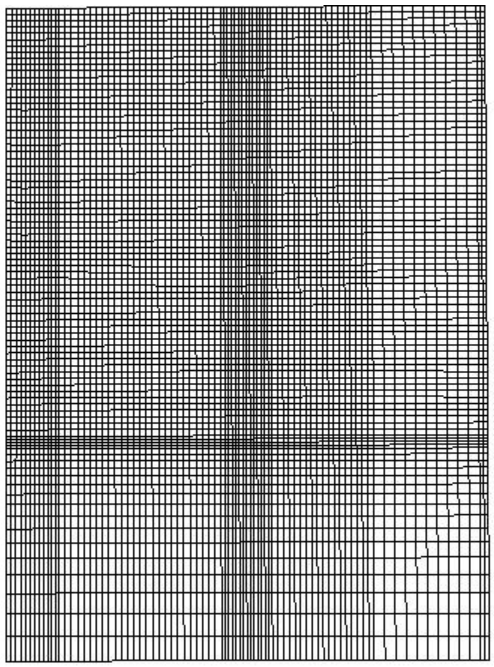

Figure 10. Grid G3 1.5 m above the floor

The difference in the mesh density between G5 and G3 can also be noted in Figure 11 and Figure 12 which show the south wall from inside looking out through the south door.

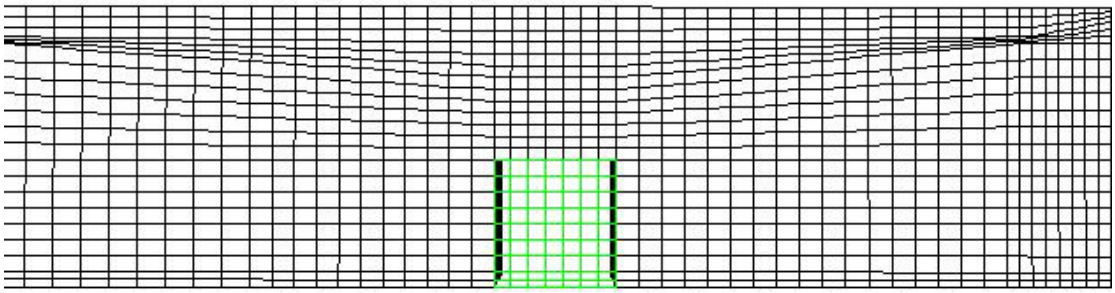

Figure 11. Grid G5 looking out through the south door

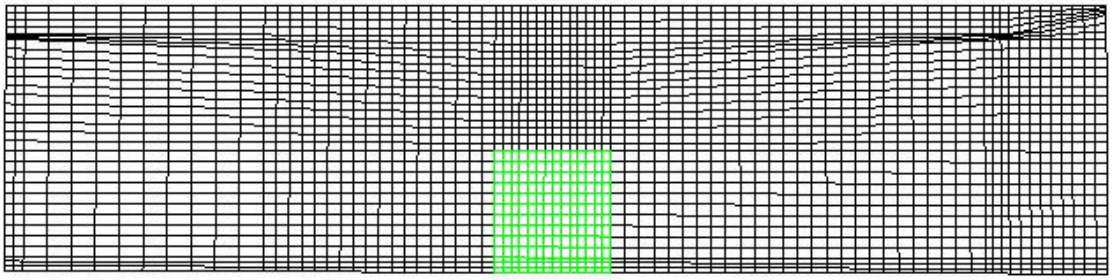

Figure 12. Grid G3 looking out through the south door

It should be noted that even though grid independency is fulfilled in the steady cases with wind speed 10 m/s it might be necessary to refine the grid when the wind speed is increased to 15 m/s or when the time dependent cases are investigated. This was not done in the present work and therefore the accuracy of the calculations can not be judged as high.

4 Results and Discussion

4.1 Grid Dependency

The results achieved for the temperature distribution in the horizontal plane 1.5 m above the floor using four different grids (cases 1 – 4) are presented in the following four figures.

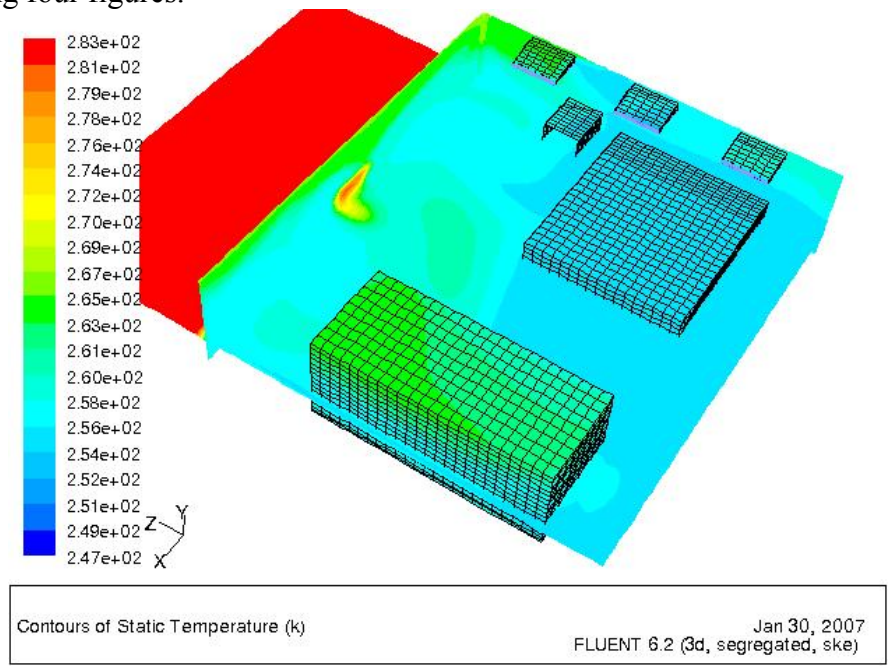

Figure 13. Temperature contours. The horizontal plane is 1.5 m above the floor. Case 1 using grid G1

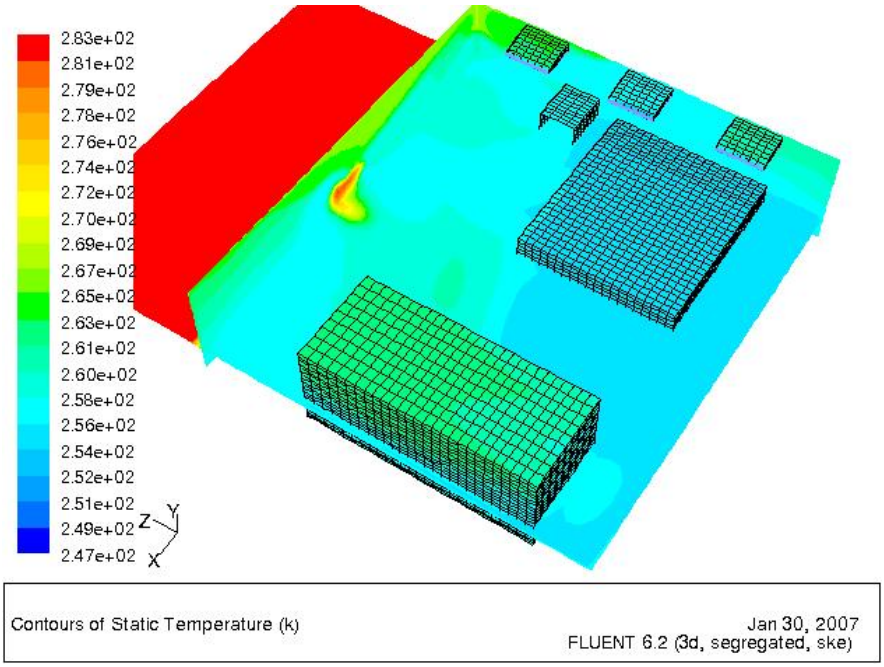

Figure 14. Temperature contours. The horizontal plane is 1.5 m above the floor. Case 2 using grid G2

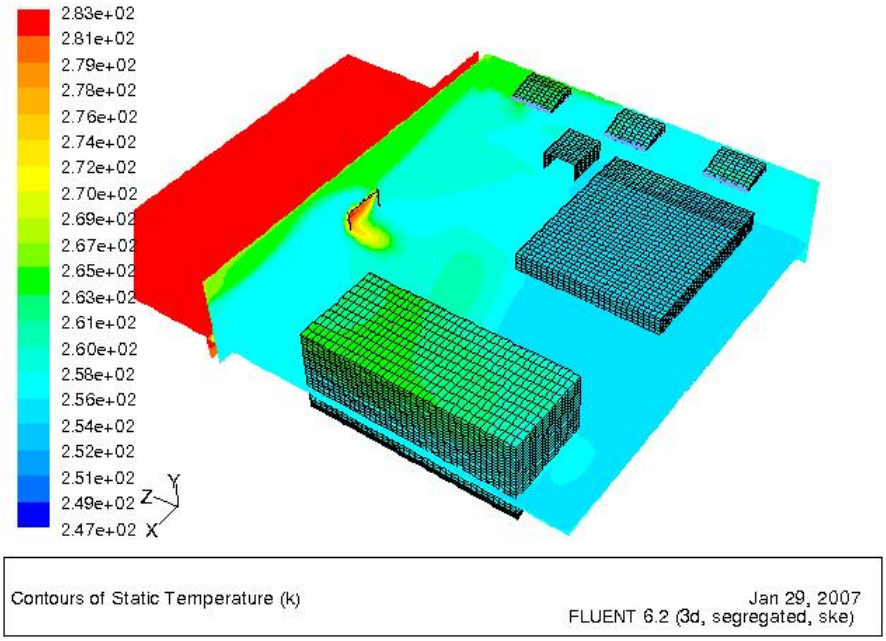

Figure 15. Temperature contours. The horizontal plane is 1.5 m above the floor. Case 3 using grid G3

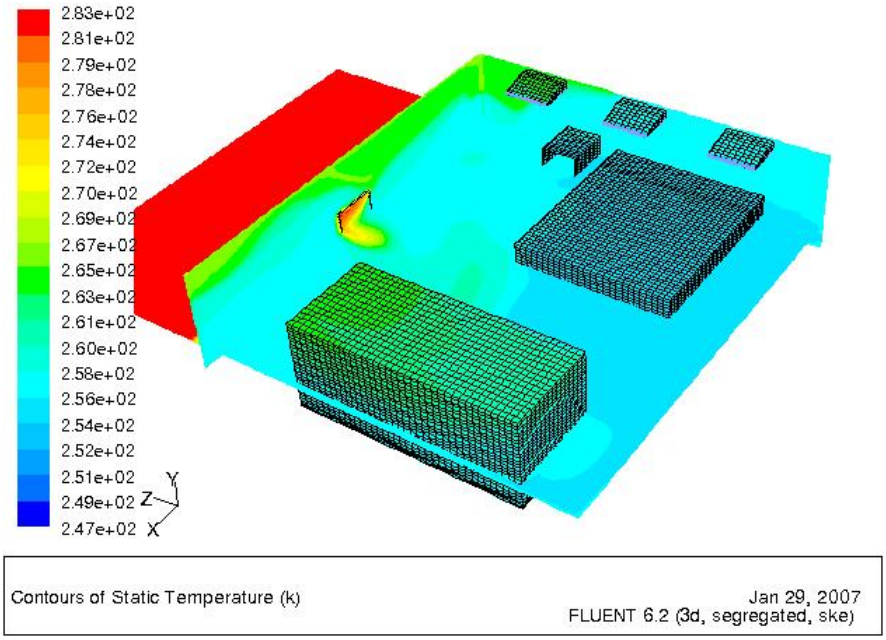

Figure 16. Temperature contours. The horizontal plane is 1.5 m above the floor. Case 4 using grid G4

Since the deviation in temperature distribution between these four cases seems reasonably small, it was decided to use the first grid, G1, in the following calculations. The underlying reason is the need to spare computational power during the calculations.

4.2 Steady Cases with South Door Closed

Before running the unsteady cases 14 – 16, the initial solutions for the unsteady cases were created by running the steady cases nr. 7 – 9. The results are shown in Figures 17 – 19.

4.2.1 Wind Speed 10 m/s

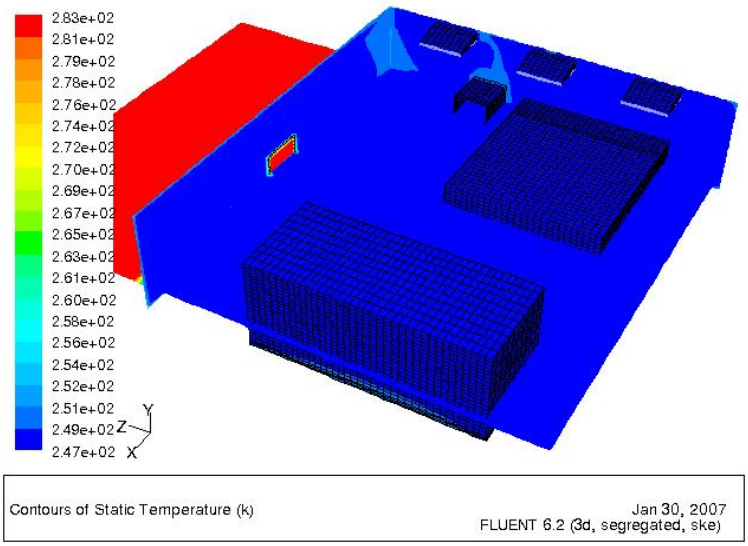

Figure 17. Temperature contours. The horizontal plane is 1.5 m above the floor. Case 7 with wind speed 10 m/s

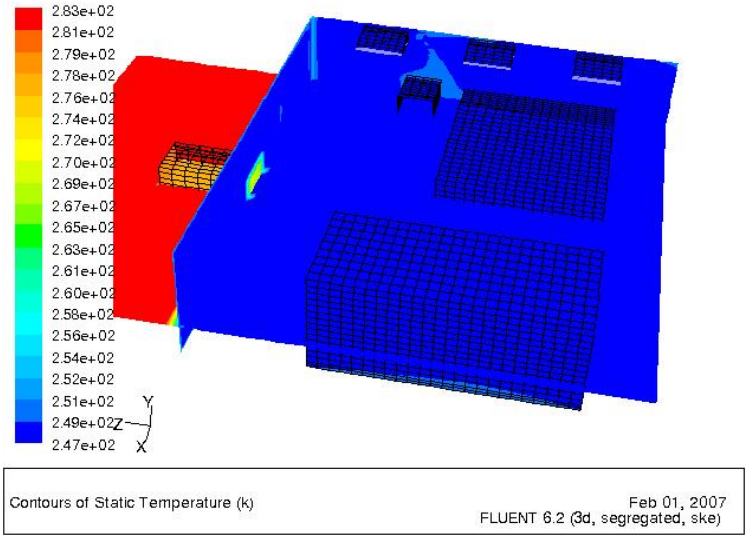

Figure 18. Temperature contours. The horizontal plane is 1.5 m above the floor. Case 10 with wind speed 10 m/s including a 4 m long hall south of the closed south door

4.2.2 No Wind

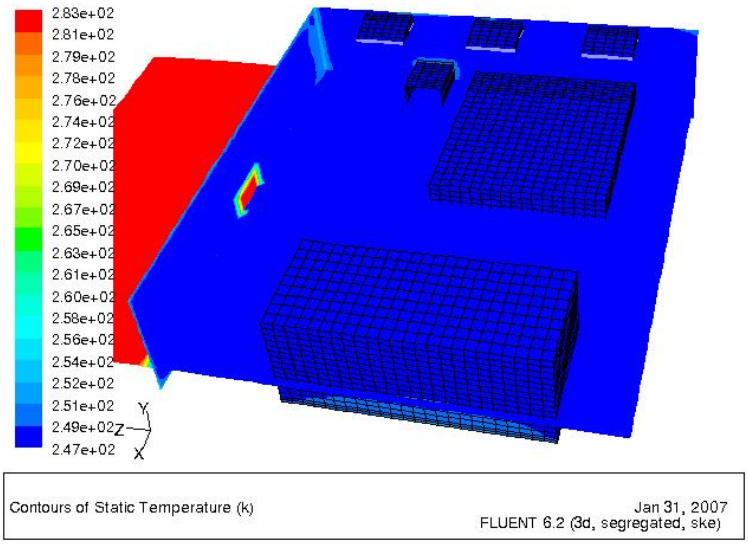

Figure 19. Temperature contours. The horizontal plane is 1.5 m above the floor. Case 8 with no wind

The temperature distribution in case 9 with wind speed of 15 m/s is not shown here since it is very similar to the results from cases 7 and 8. These temperature distributions can be compared to the measured temperature distribution by Hlynur Þór Björnsson [6]. However, there are few aspects that make it harder to compare the calculated results with the measured ones. These aspects are among others:

- Uncertainty about the weather conditions while the measurements were done. As earlier said, in the present study a southerly wind (of different strength) is assumed. The temperature of 10 °C (283 K) is also accepted since it is the average temperature during the summertime in Iceland, when the measurements were done.
- Uncertainty about the frequency and length of the door openings (both the south door and the west door – in this work only opening of the south door is investigated).
- Uncertainty of how much frozen fish was found in the freeze room during the measurements and also the location of it. It's not hard to imagine that the existence of frozen fish can have noticeable effect on the air flow and thereby temperature distribution in the freeze room.
- Quite few temperature loggers were used for measuring the temperature distribution; the number of loggers was only between 20 – 30 according to [6] and only half of it located at the 1.5 m level above the floor. The rest was placed close to the roof but no results from these temperature investigations are presented here.

Figure 20 presents the temperature distribution 1.5 m above the floor as measured during night time. Judging by the figure the temperature is below -20 °C (253 K) in large part of the plane just as in Figure 17 and Figure 19. However, noticeable difference is seen close to the south wall, where the CFD calculations seem to under predict the temperature compared to the measurements.

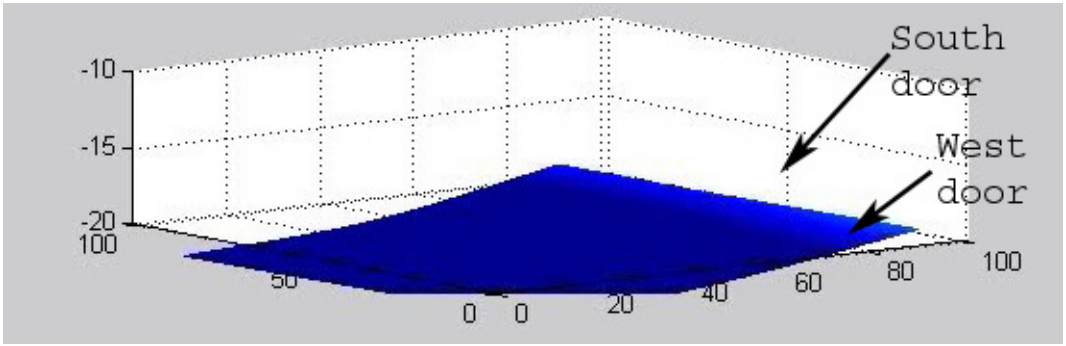

Figure 20. Measured temperature distribution in the freeze room. The vertical axis shows the temperature in °C and the horizontal plane represents the plane 1.5 m above the floor. The arrows show the approximate locations of the two doors

4.3 Steady Cases with South Door Open

The cases with the south door open should be viewed as some kind of worst case scenario since in reality; the door is only open for a certain time when frozen fish is transferred through it. The number of openings is also limited and of course very different, depending on the quantity of the fish transfer.

4.3.1 No Wind

In Figure 21 the temperature distribution in case 5 with no southerly wind can be seen. Comparison to Figure 19 (case 8 with no wind but the door closed) implies that leaving the south door open for a long time doesn't significantly increase the temperature in the freeze room, assumed that no wind is blowing. In most of the investigated plane, 1.5 m above the floor, the temperature increase is around 2 – 4 °C and the increase is noticeably larger very close to the south wall.

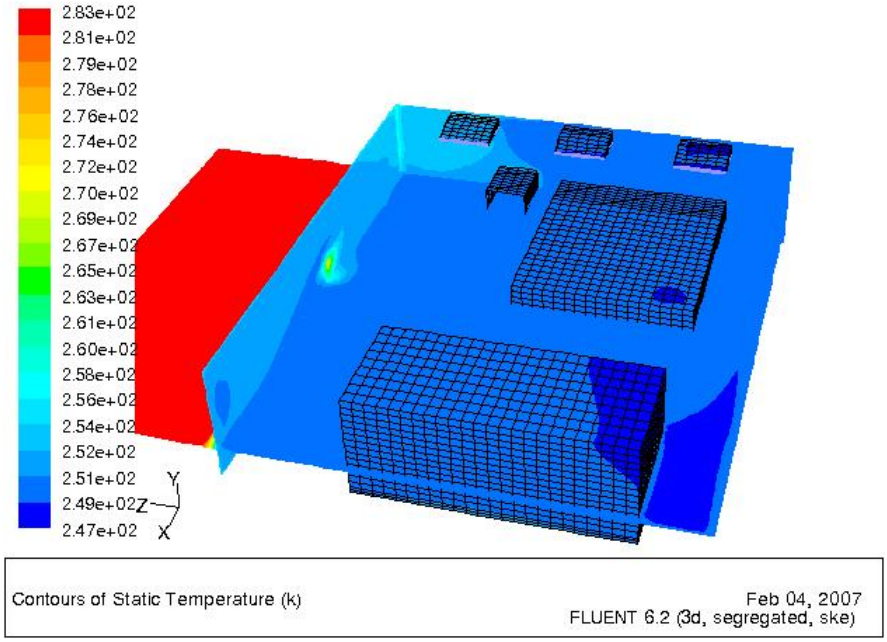

Figure 21. Temperature contours. The horizontal plane is 1.5 m above the floor. Case 5 with no southerly wind

4.3.2 Wind Speed 10 m/s

Figure 22 presents the corresponding result for case 10 as Figure 13 does for case 1; the difference is that case 10 includes a 4 m long and open hall south of the south door.

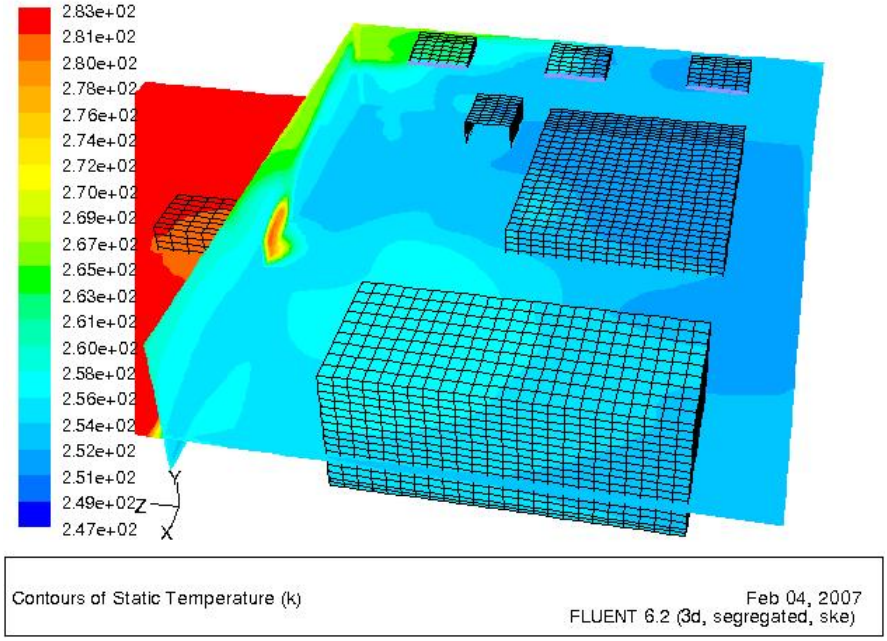

Figure 22. Temperature contours. The horizontal plane is 1.5 m above the floor. Case 10 with southerly wind of 10 m/s including a 4 m long hall in front of the south door

By comparing the two figures it can be stated that the addition of the hall results in around 2 – 6 °C temperature decrease, depending on the location. The difference seems to be even larger when the temperature distribution close to the roof (in the height of the openings of the air ducts) is inspected. This can be seen by comparing Figure 23 and Figure 24 below.

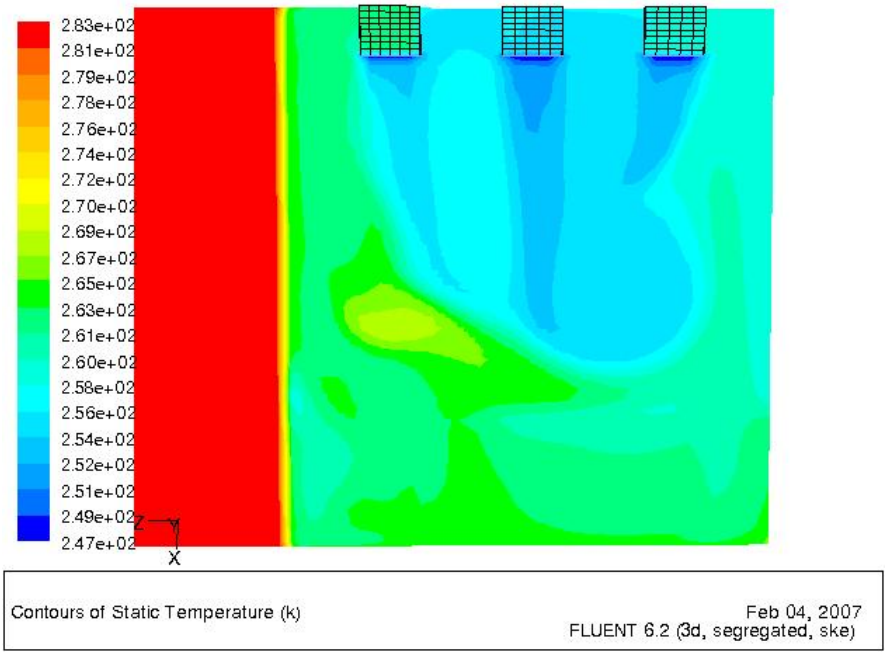

Figure 23. Temperature contours in the height of the refrigerating units close to the roof. Case 1 with southerly wind of 10 m/s without a hall in front of the south door

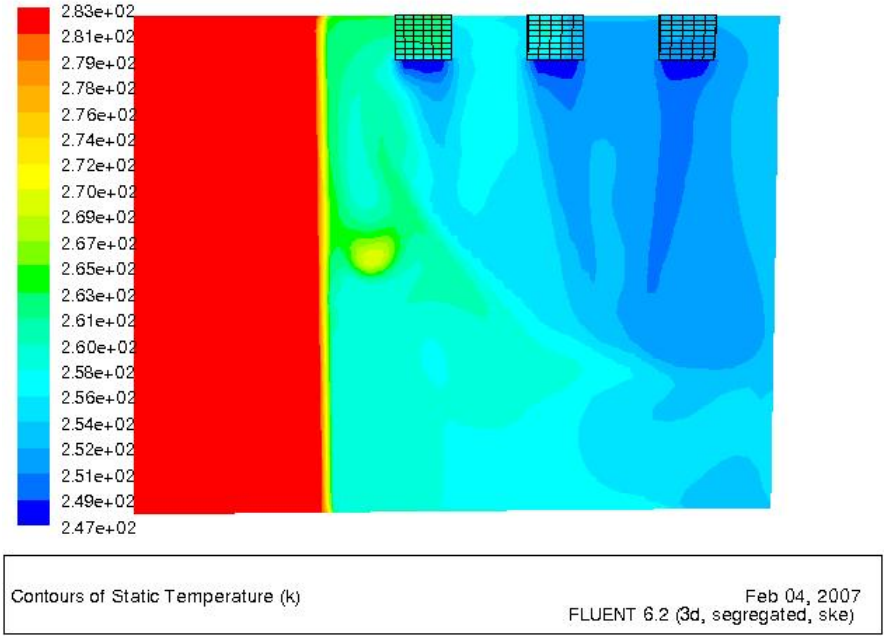

Figure 24. Temperature contours in the height of the refrigerating units close to the roof. Case 10 with southerly wind of 10 m/s including a 4 m long hall in front of the south door

4.3.3 Wind Speed 15 m/s

When the results for case 6 (see Figure 25) are compared to the results from case 1 (see Figure 13) higher average temperature can be noted in the freeze room in the former case. Still, more obvious are the effects of placing the south hall (tunnel) in front of the south door as is done in case 11. Temperature distribution for case 11

is presented in Figure 26 and it should be compared to Figure 25 to observe the influence of the south hall.

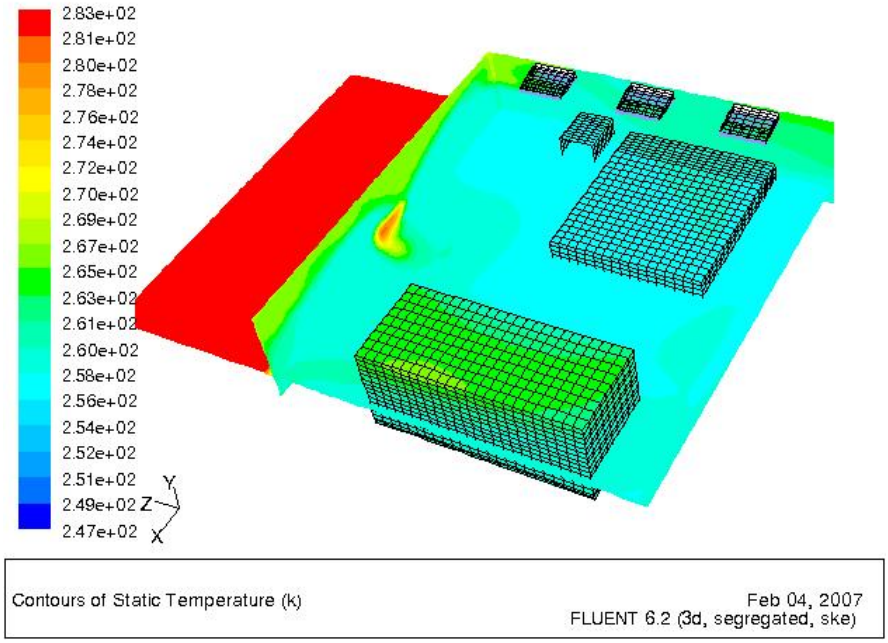

Figure 25. Temperature contours. The horizontal plane is 1.5 m above the floor. Case 6 with southerly wind of 15 m/s

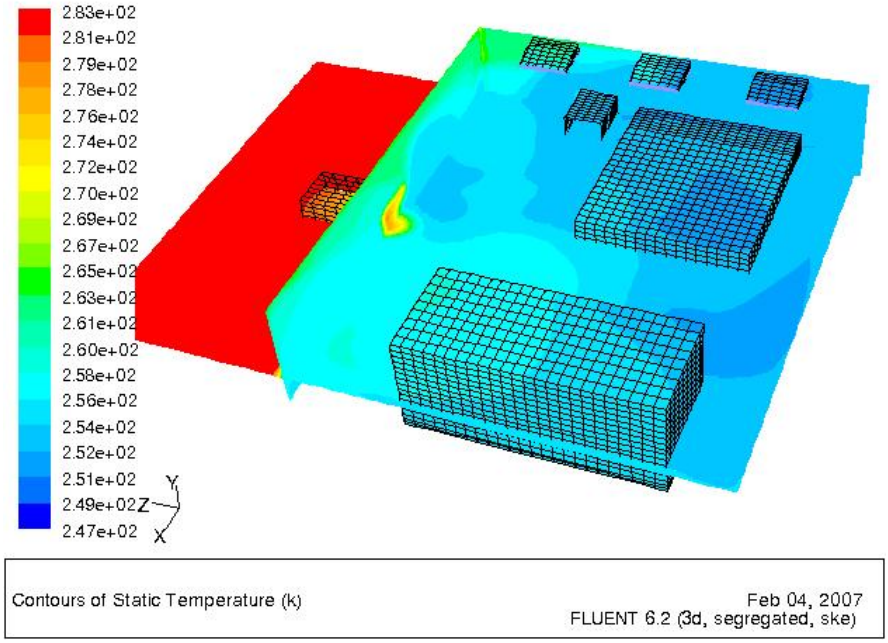

Figure 26. Temperature contours. The horizontal plane is 1.5 m above the floor. Case 11 with southerly wind of 15 m/s including a 4 m long hall in front of the south door

The influence of the south hall is also evident when the temperature distribution is investigated close to the roof. Figure 27 and Figure 28 present results for case 6 (without the hall) and case 11 (including the hall), respectively, and comparison of the two figures makes the influence clear.

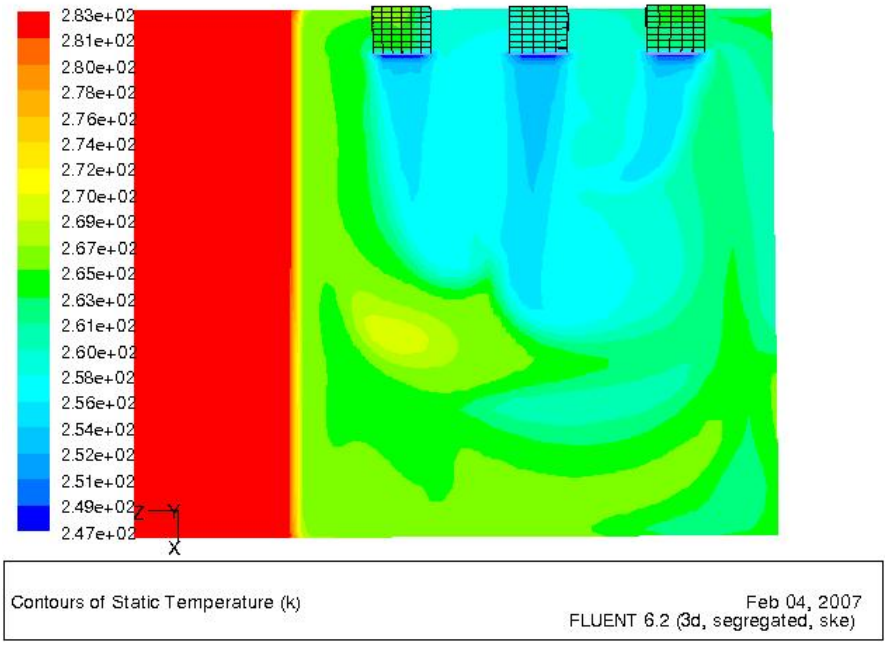

Figure 27. Temperature contours in the height of the refrigerating units close to the roof. Case 6 with southerly wind of 15 m/s without a hall in front of the south door

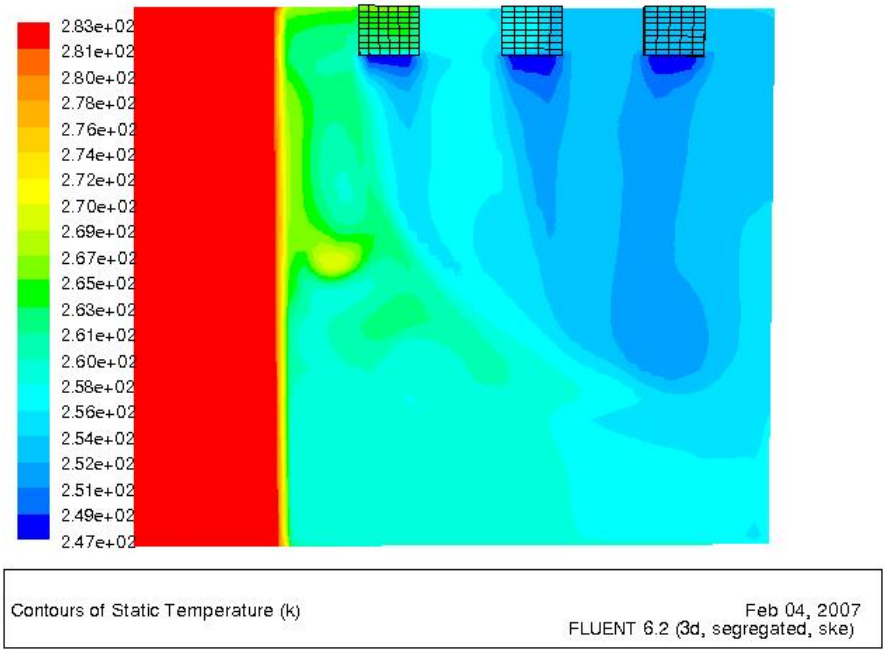

Figure 28. Temperature contours in the height of the refrigerating units close to the roof. Case 11 with southerly wind of 15 m/s including a 4 m long hall in front of the south door

4.4 Unsteady Cases with South Door Open

The results for the time dependent cases are presented in sequences of figures with 10 - 20 seconds between each two consecutive figures (snap shots) except the first figure in each sequence is taken 0.5 seconds after the door has been opened. The time step size in the calculations was 0.5 seconds so only a part of the results are presented in this report. The whole set of figures for each case was used to make movies (on mpeg - and wmv - formats), which is a nice way to illustrate how the temperature changes as time goes by but can not be presented here.

4.4.1 Wind Speed 10 m/s

The sequence in Figure 29 shows how the temperature in the freeze room evolves for the first two minutes in case 14 (no south hall included and the wind speed is 10 m/s). The time interval between two consecutive figures is 10 seconds. After two minutes opening, temperature between -19 and -15 °C can be found in large domains which can not been judged as satisfactory.

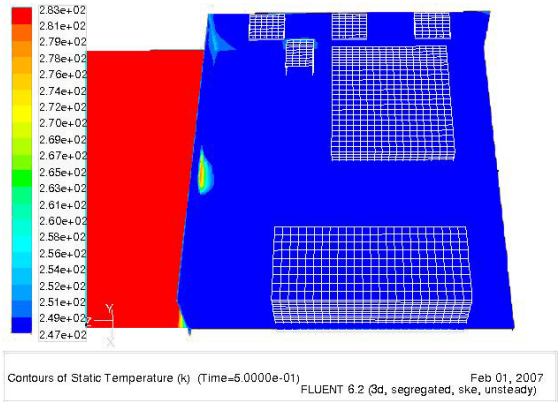

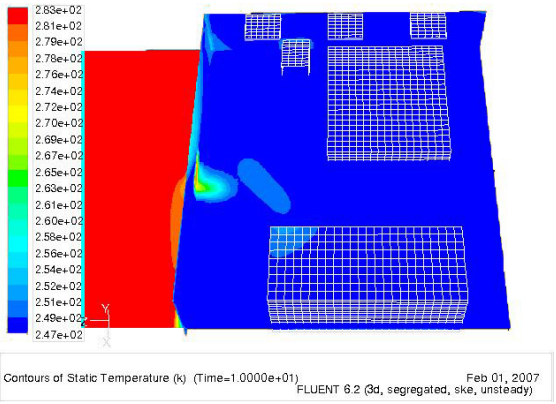

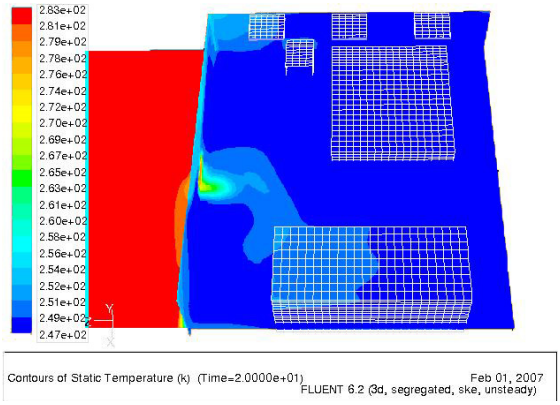

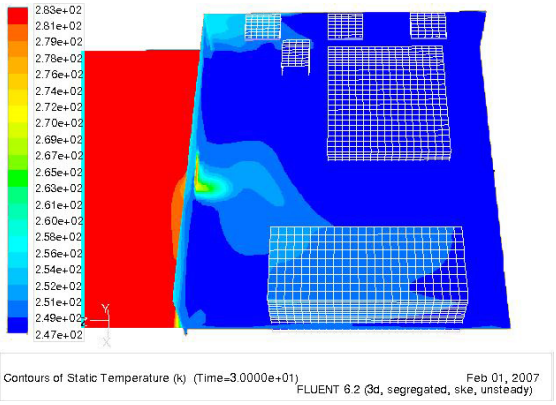

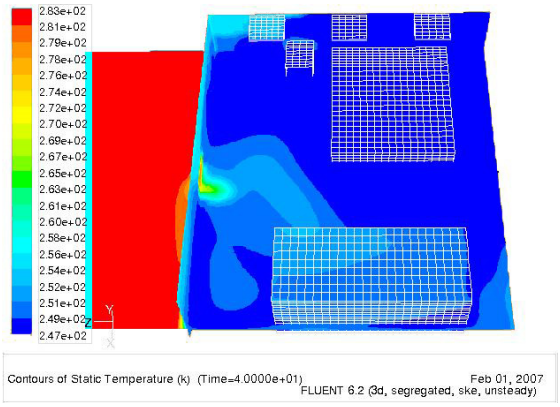

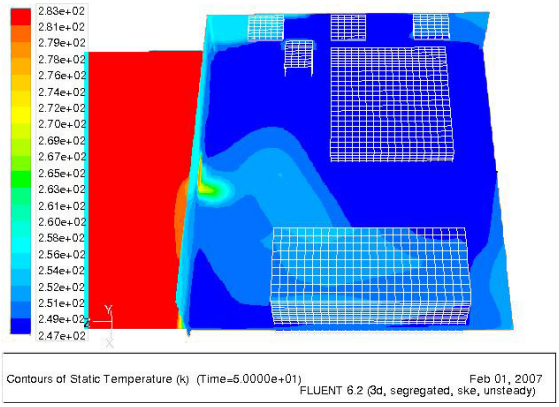

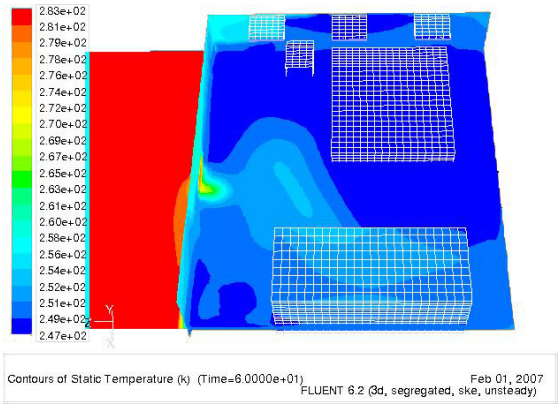

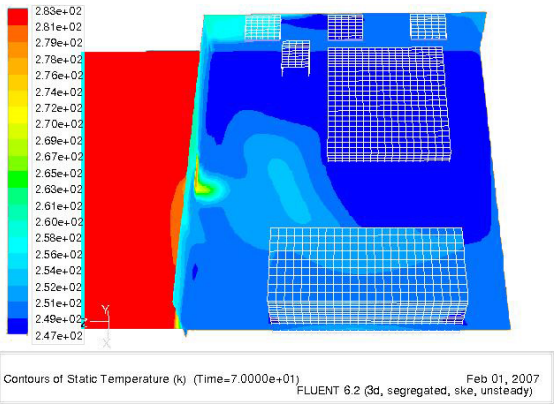

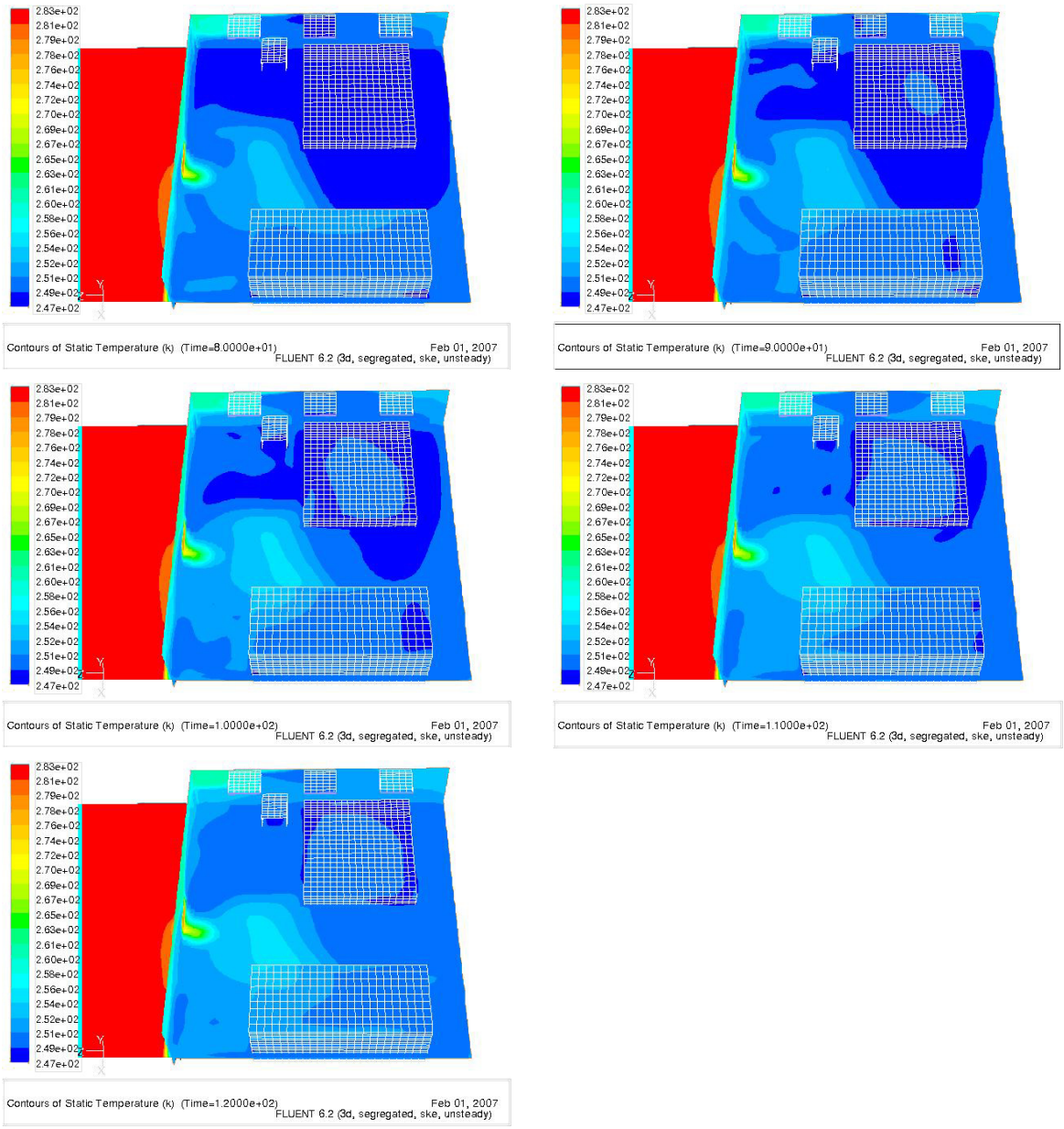

Figure 29. Temperature evolution for the first 2 minutes after the south door is opened in case 14. The horizontal plane is 1.5 m above the floor. The south hall is not included and the wind speed is 10 m/s. Time is shown in seconds below each snap shot

In order to validate the results for the temperature evolution in the figure above some results from the measurements are presented in a figure sequence in Figure 30. The figure shows how the temperature evolves over an unknown time period during the daytime. During the day the doors (both south and west doors) are opened, therefore the temperature increase in the freeze room that can be noticed in the fore mentioned figure. As has already been pointed out in Chapter 4.2.2, it is very hard to compare the CFD results with the measured one but it can still be noted in Figure 30 that the temperature increase definitely occurs first close to the south wall and then spreads out. The same trend is witnessed in the CFD results in Figure 29 and also in the other figures to come from the unsteady cases in the present study.

The last snap shots in Figure 30 show the temperature evolution as the doors have been closed again but this case was not inspected in the present work. Unsurprisingly, the high temperature is longest lasting in the south-west corner between the two doors.

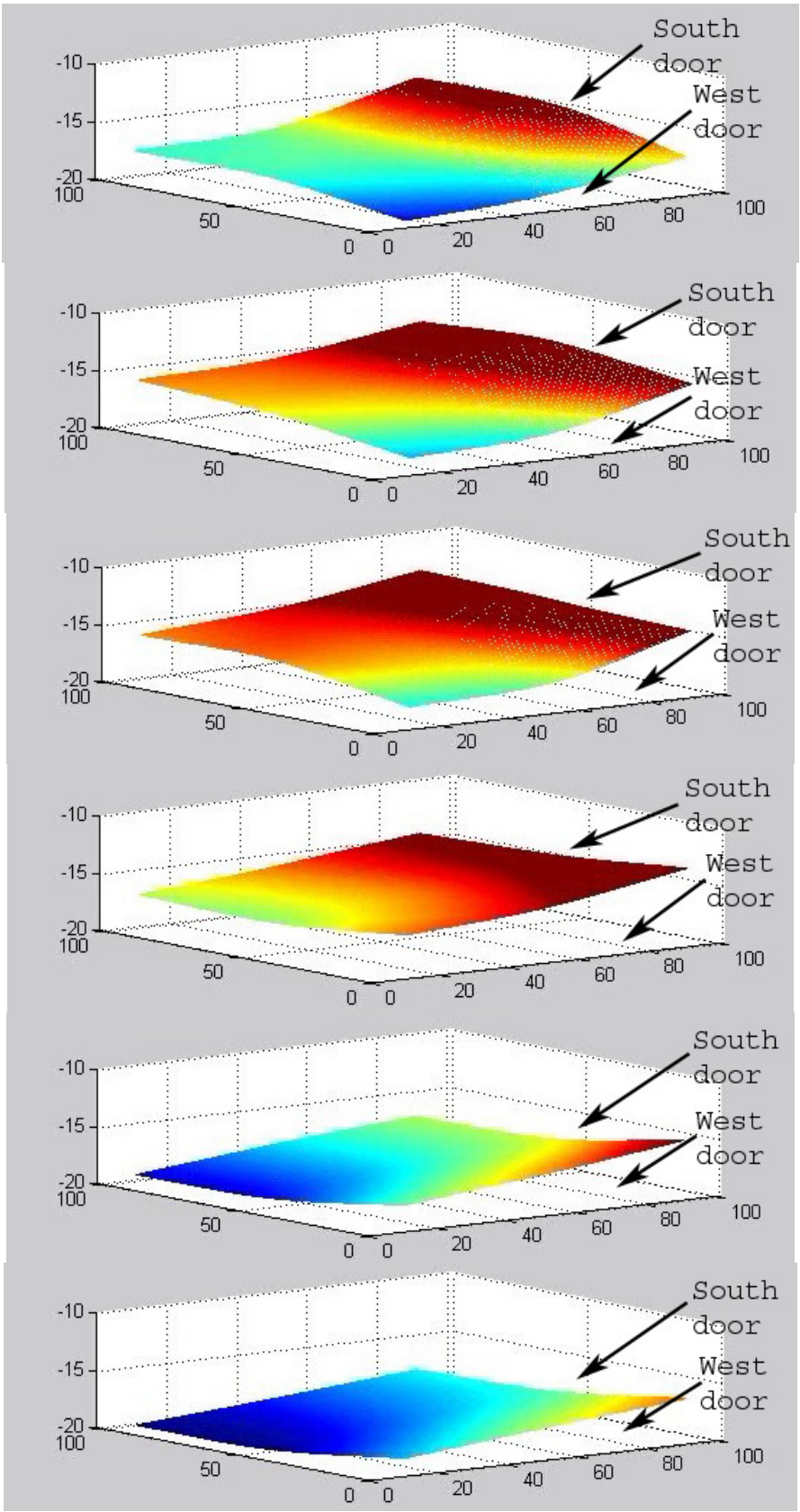

Figure 30. Evolution of the measured temperature distribution in the freeze room. The vertical axis shows the temperature in °C and the horizontal plane represents the plane 1.5 m above the floor. The arrows show the approximate locations of the two doors

When the south hall is added the CFD results change considerably as can be seen in Figure 31 below. When the two solutions (with and without the south hall) after 2 minutes are compared it can be noted that in the latter case the blue color domain, representing the temperature level 247 K – 249 K (between -26 °C and -24 °C) is significantly larger and also the green color representing 261 K – 267 K doesn't reach as long into the freeze room. This in spite of the fact that no closed doors were added to the model, only an open hall, basically an open 4 m long tunnel, in front of the south door.

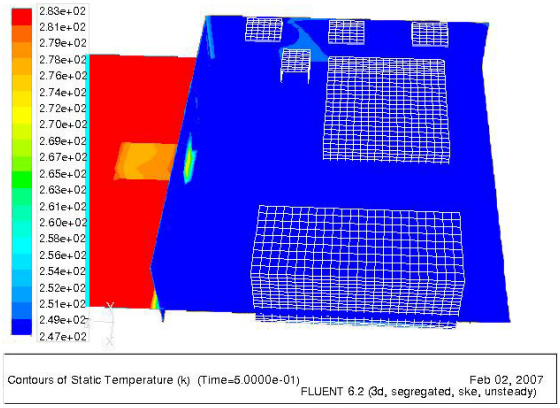

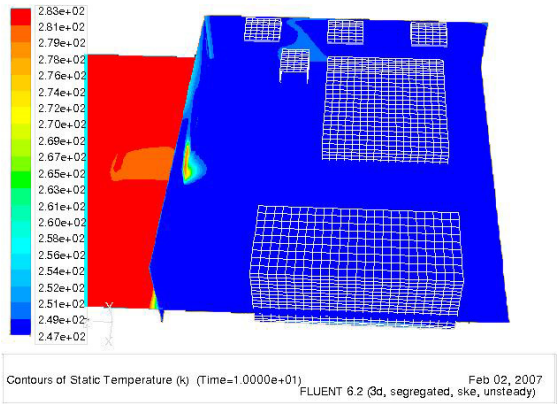

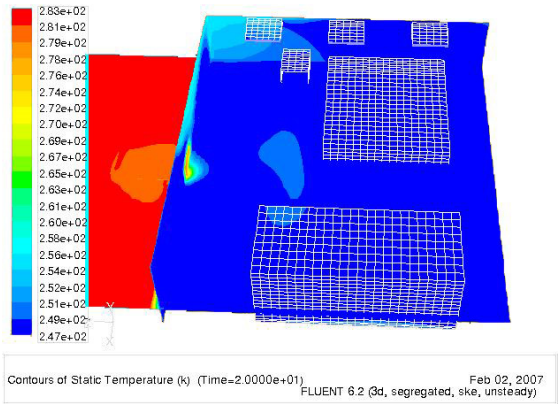

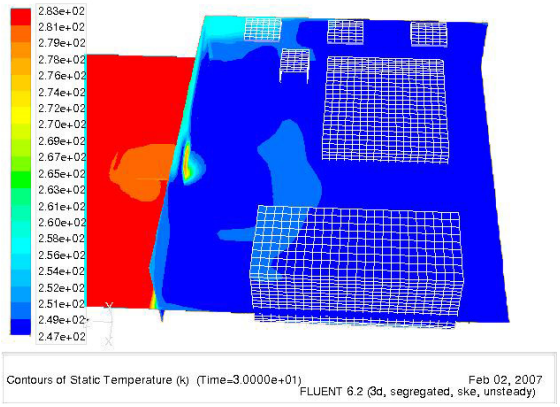

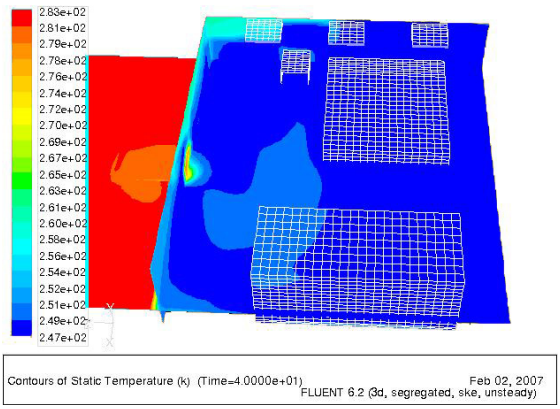

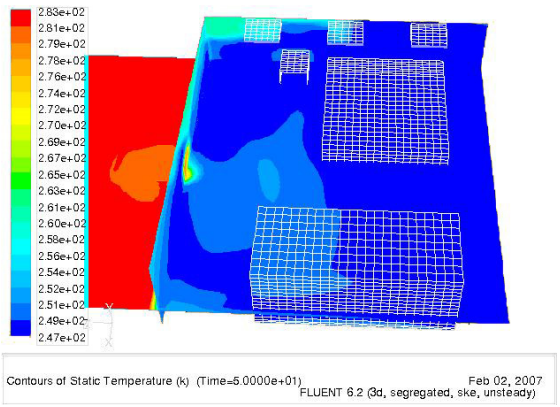

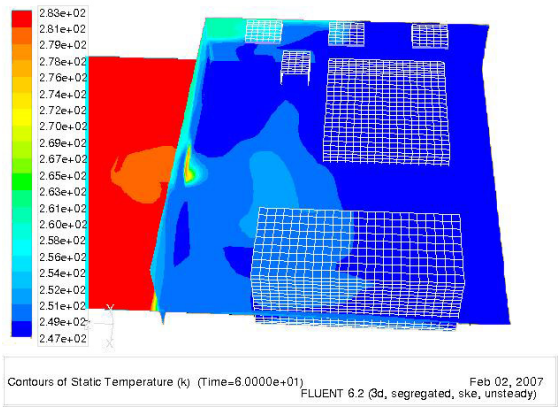

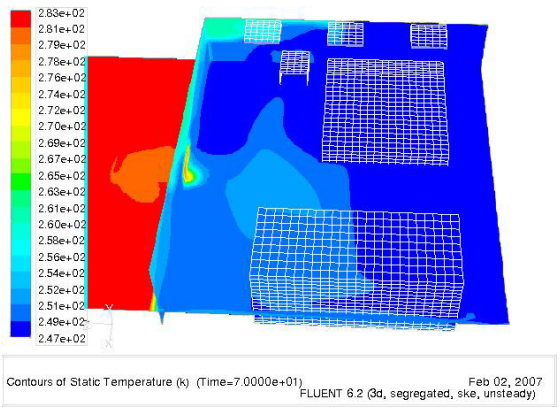

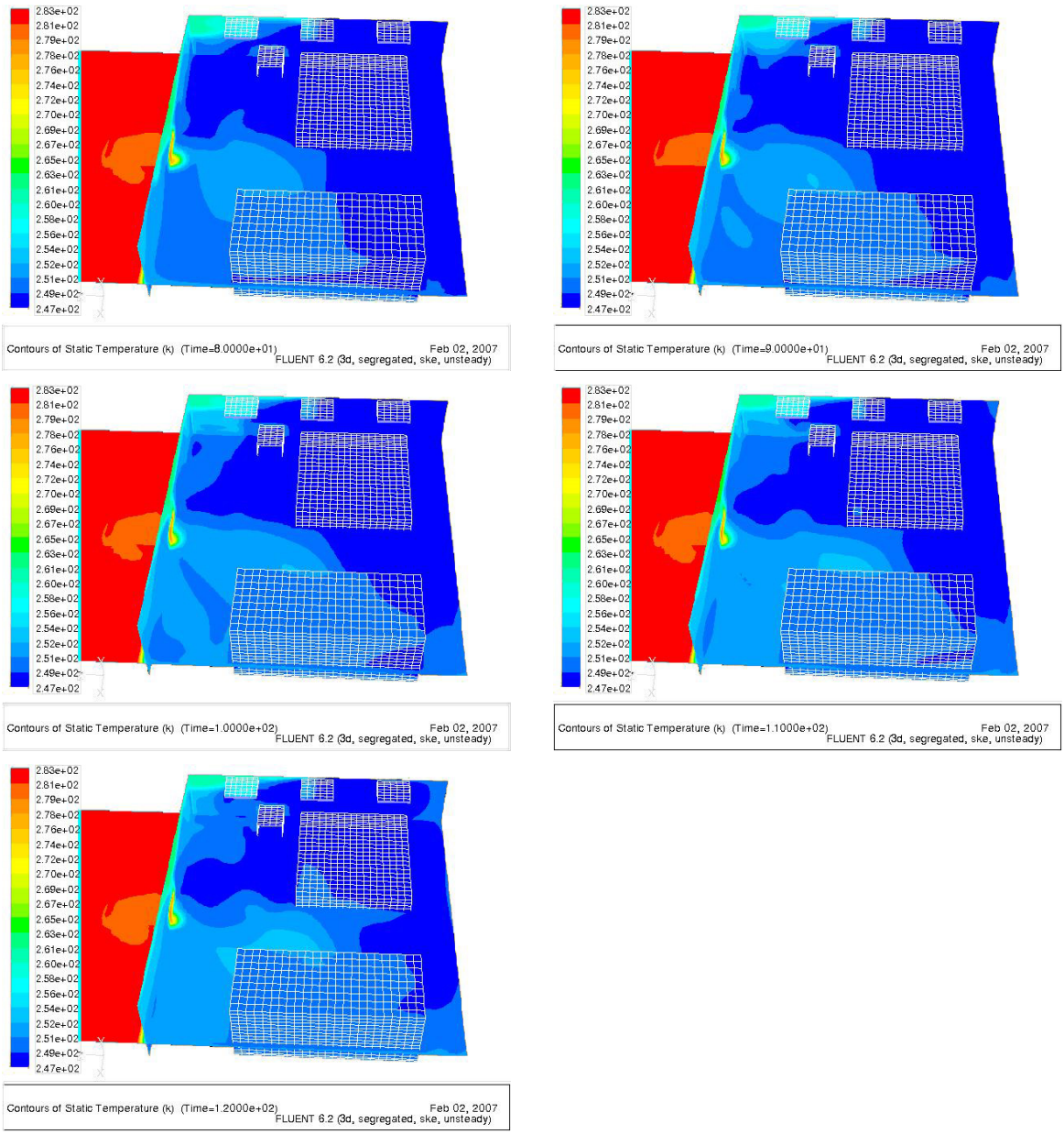

Figure 31. Temperature evolution for the first 2 minutes after the south door is opened in case 16. The horizontal plane is 1.5 m above the floor. The south hall is included and the wind speed is 10 m/s. Time is shown in seconds below each snap shot

The influence of the south hall can once again been noticed by comparing Figure 32 and Figure 33 which show the temperature 3 m above the floor instead of 1.5 m as before. The former figure shows the temperature distribution when no south hall is used (case 14) and the latter shows the temperature distribution from a slightly rotated view with the south hall included (case 16).

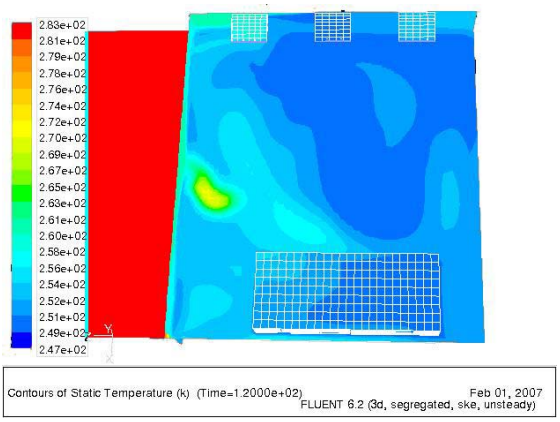

Figure 32. Temperature distribution 2 minutes after the south door is opened in case 14. The horizontal plane is 3 m above the floor. The south hall is not included and the wind speed is 10 m/s

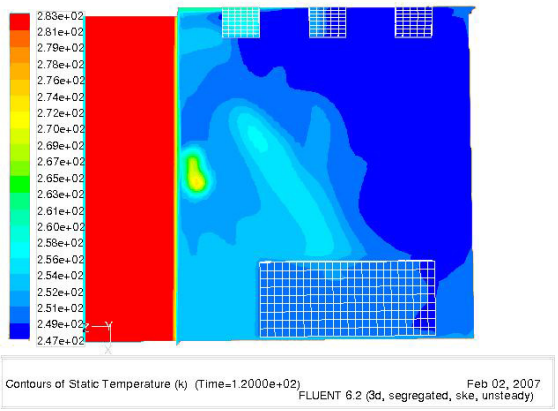

Figure 33. Temperature distribution 2 minutes after the south door is opened in case 16. The horizontal plane is 3 m above the floor. The south hall is included and the wind speed is 10 m/s

4.4.2 Wind Speed 15 m/s

The snap shot sequence in Figure 34 shows how the temperature in the freeze room evolves for the first two minutes in case 15 (no south hall included and wind speed of 15 m/s). The time interval between two consecutive figures is 20 seconds. When the solution after 2 minutes for case 15 is compared to the corresponding case with wind speed of 10 m/s, i.e. case 14, it can be judged from the overall temperature distribution that the wind speed plays a significant role. It can also be seen from Figure 34 that already 4 minutes after the south door is opened the temperature has reached the level of -19 to -13 °C almost everywhere in the plane 1.5 m above the floor.

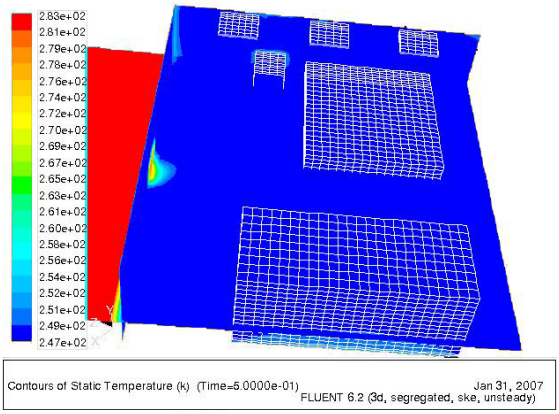

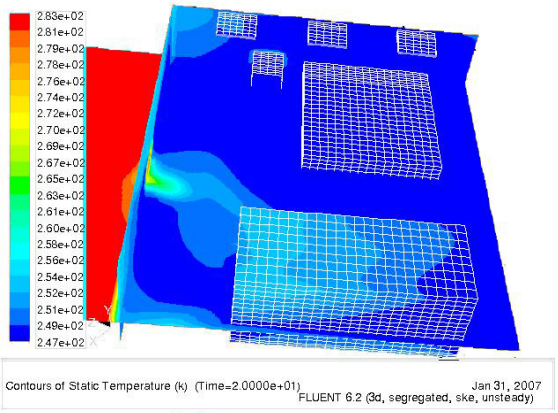

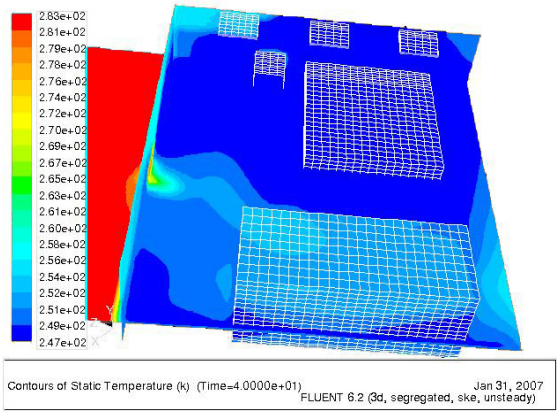

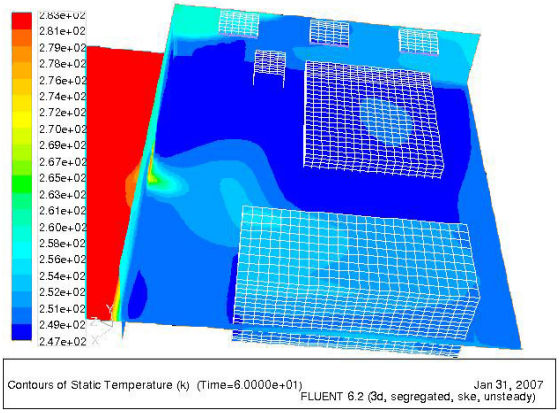

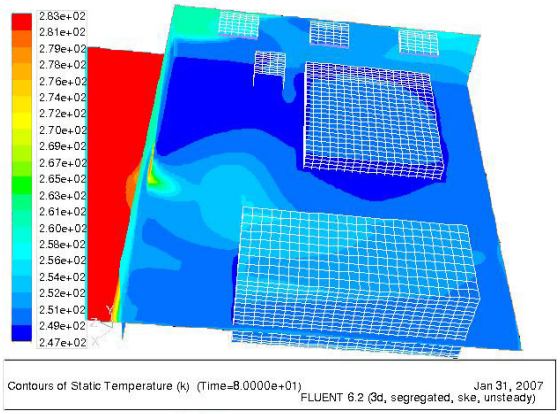
2.83e+02
2.81e+02
2.79e+02
2.78e+02
2.76e+02
2.74e+02
2.72e+02
2.70e+02
2.69e+02
2.67e+02
2.65e+02
2.63e+02
2.61e+02
2.60e+02
2.58e+02
2.56e+02
2.54e+02
2.52e+02
2.51e+02
2.49e+02
2.47e+02
Contours of Static Temperature (k) (Time=8.0000e+01)
Jan 31, 2007
FLUENT 6.2 (3d, segregated, ske, unsteady)

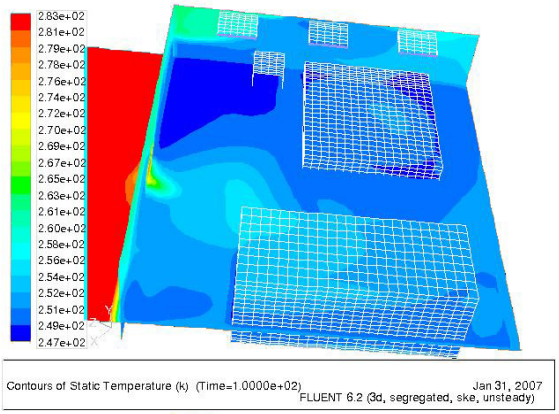
2.83e+02
2.81e+02
2.79e+02
2.78e+02
2.76e+02
2.74e+02
2.72e+02
2.70e+02
2.69e+02
2.67e+02
2.65e+02
2.63e+02
2.61e+02
2.60e+02
2.58e+02
2.56e+02
2.54e+02
2.52e+02
2.51e+02
2.49e+02
2.47e+02
Contours of Static Temperature (k) (Time=1.0000e+02)
Jan 31, 2007
FLUENT 6.2 (3d, segregated, ske, unsteady)

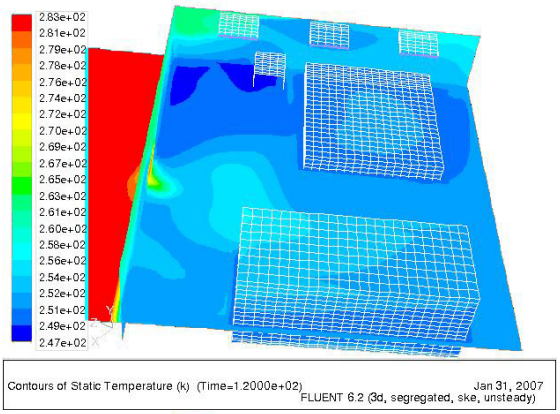
2.83e+02
2.81e+02
2.79e+02
2.78e+02
2.76e+02
2.74e+02
2.72e+02
2.70e+02
2.69e+02
2.67e+02
2.65e+02
2.63e+02
2.61e+02
2.60e+02
2.58e+02
2.56e+02
2.54e+02
2.52e+02
2.51e+02
2.49e+02
2.47e+02
Contours of Static Temperature (k) (Time=1.2000e+02)
Jan 31, 2007
FLUENT 6.2 (3d, segregated, ske, unsteady)

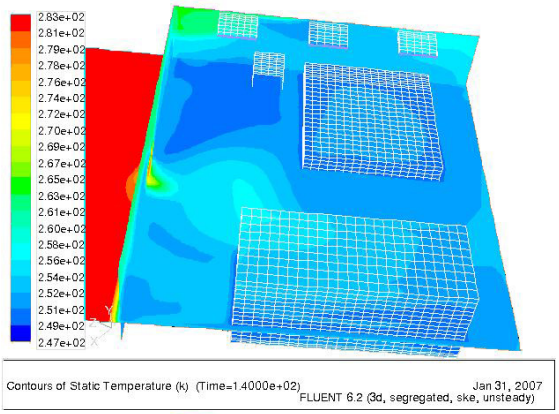
2.83e+02
2.81e+02
2.79e+02
2.78e+02
2.76e+02
2.74e+02
2.72e+02
2.70e+02
2.69e+02
2.67e+02
2.65e+02
2.63e+02
2.61e+02
2.60e+02
2.58e+02
2.56e+02
2.54e+02
2.52e+02
2.51e+02
2.49e+02
2.47e+02
Contours of Static Temperature (k) (Time=1.4000e+02)
Jan 31, 2007
FLUENT 6.2 (3d, segregated, ske, unsteady)

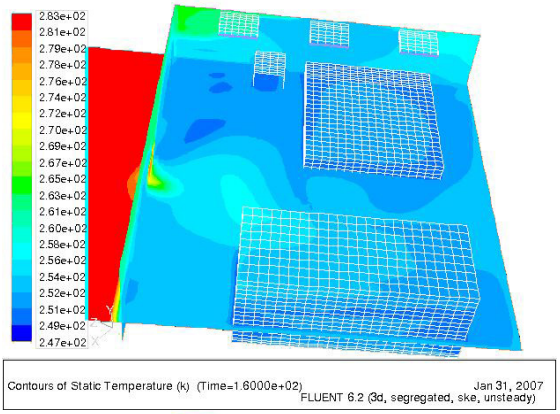
2.83e+02
2.81e+02
2.79e+02
2.78e+02
2.76e+02
2.74e+02
2.72e+02
2.70e+02
2.69e+02
2.67e+02
2.65e+02
2.63e+02
2.61e+02
2.60e+02
2.58e+02
2.56e+02
2.54e+02
2.52e+02
2.51e+02
2.49e+02
2.47e+02
Contours of Static Temperature (k) (Time=1.6000e+02)
Jan 31, 2007
FLUENT 6.2 (3d, segregated, ske, unsteady)

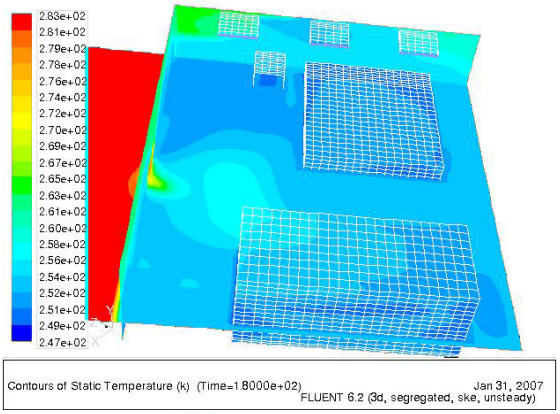
2.83e+02
2.81e+02
2.79e+02
2.78e+02
2.76e+02
2.74e+02
2.72e+02
2.70e+02
2.69e+02
2.67e+02
2.65e+02
2.63e+02
2.61e+02
2.60e+02
2.58e+02
2.56e+02
2.54e+02
2.52e+02
2.51e+02
2.49e+02
2.47e+02
Contours of Static Temperature (k) (Time=1.8000e+02)
Jan 31, 2007
FLUENT 6.2 (3d, segregated, ske, unsteady)

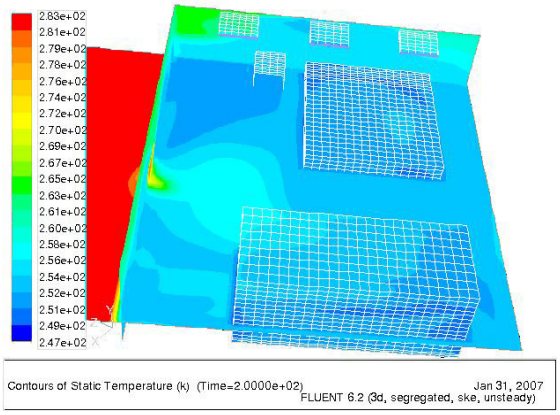
2.83e+02
2.81e+02
2.79e+02
2.78e+02
2.76e+02
2.74e+02
2.72e+02
2.70e+02
2.69e+02
2.67e+02
2.65e+02
2.63e+02
2.61e+02
2.60e+02
2.58e+02
2.56e+02
2.54e+02
2.52e+02
2.51e+02
2.49e+02
2.47e+02
Contours of Static Temperature (k) (Time=2.0000e+02)
Jan 31, 2007
FLUENT 6.2 (3d, segregated, ske, unsteady)

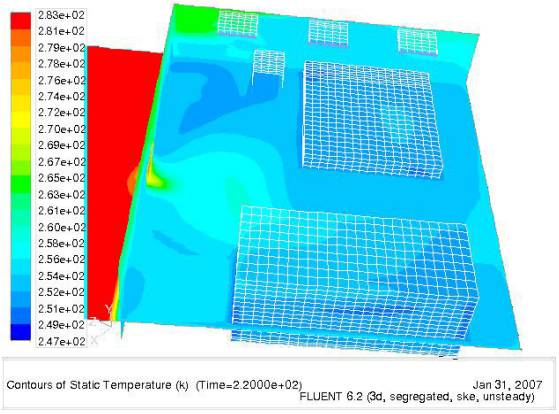
2.83e+02
2.81e+02
2.79e+02
2.78e+02
2.76e+02
2.74e+02
2.72e+02
2.70e+02
2.69e+02
2.67e+02
2.65e+02
2.63e+02
2.61e+02
2.60e+02
2.58e+02
2.56e+02
2.54e+02
2.52e+02
2.51e+02
2.49e+02
2.47e+02
Contours of Static Temperature (k) (Time=2.2000e+02)
Jan 31, 2007
FLUENT 6.2 (3d, segregated, ske, unsteady)

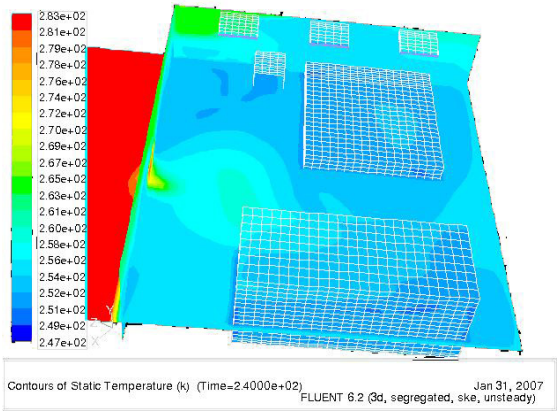

Figure 34. Temperature evolution for the first 4 minutes after the south door is opened in case 15. The horizontal plane is 1.5 m above the floor. The south hall is not included and the wind speed is 15 m/s. Time is shown in seconds below each snap shot

5 Conclusions and Future Work

According to the computational simulations, presented in this report, the addition of an open hall south of the south door is very important in order to decrease the negative effects of southerly wind blowing through an open south door. The temperature increase in the freeze room is definitely not as much if the hall is included, even though the hall is open in both ends. Another main result of the calculations is the strong influence of the wind speed, which seems, however, to be weakened seriously by adding the hall.

As earlier noted, comparison with the measurements that were done on the temperature distribution in the freeze room, was very difficult mainly because of several uncertainties concerning the measurements. Still, some correspondence can be found between the CFD results and the measurements, both by looking at the steady and the unsteady cases. Therefore, it can be stated that the model developed is a trustworthy design tool, at least in order to give a rough estimate of the influence of changed weather circumstances or changes in the building design.

Future work might include some accurate temperature measurements in order to validate the calculated results better. Of course, these measurements have to be performed in the same circumstances as were adopted in the present work to be useful for validation.

Concerning the numerical simulations, it should be mentioned that careful investigation of turbulence properties close to doors and surfaces would most likely crave a lot finer grids than were used in this study.

References

1. Alhama, F., González Fernandez, C. F., Zueco, F. 2004. Inverse determination of the specific heat of foods. Journal of Food Engineering, 64, p. 347 – 353.

2. Flick, D., Moureh, J., 2004. Air pattern and temperature distribution in a typical refrigerated truck configuration loaded with pallets. International Journal of Refrigeration, 27, p. 464 – 474.

3. Fluent Manual. www.fluent.com

4. Geankoplis C.J. 1993. Transport Processes and Unit Operations 3rd edition Prentice-Hall, New Jersey, USA

5. HB Grandi hf. Retrieved January 28th 2007, from http://hbgrandi.is/

6. Hlynur Þór Björnsson. 2005. Geymslu- og flutningastýring lausfrystra sjávarafurða. M.Sc. Thesis. University of Iceland.

7. Hoang, ML., Verboven, P, De Baermaeker, J., Nicolai, BM. 2000. Analysis of air flow in a cold store by means of computational fluid dynamics. International Journal of Refrigeration, p. 127 – 140.

8. Holman, J.P. 2002. Heat Transfer, 9th edition. McGraw-Hill, New York, USA.

9. Igarashi, T., 1986. Fluid flow and heat transfer around rectangular cylinders (the case of a width/height ratio of a section of 2.0-4.0). Trans. Jpn. Soc. Mech. Engrs., p. 3011-3016.

10. Igarashi, T., 2001. Fluid flow and heat transfer around rectangular cylinders (the case of a width/height ratio of a section of 5). International Journal of Heat and Fluid Flow, 22, p. 279 – 286.

11. Lienhard, J. H. IV, Lienhard, J. H. V, 2005. A heat transfer textbook, 3rd edition. Phlogiston Press, Cambridge, Massachusetts, USA.

12. Lunde, P. J., 1980. Solar Thermal Engineering. John Wiley and Sons, New York, USA.

13. Nilsson, Håkan. 2006. Overview of heat transfer. Lecture notes from the course MTF112. http://www.student.chalmers.se/hp/hp?hp_id=1918 Chalmers University of Technology.

14. Sartori, E., 2006. Convection coefficient equations for forced air flow over flat surfaces. Solar Energy, 80, p. 1063 – 1071.

15. Sharples, S., Charlesworth, P. S., 1998. Full scale measurements of wind-induced convective heat transfer from a roof mounted flat plate solar collector. Solar Energy, 60, p. 69 – 78.

16. Van Gerwen, RJM., Van Ort, H. Optimization of cold store using fluid dynamics models. 1990. Proceedings I.I.F. – I.I.R. Commissions B2, C2, D1, D2/3, Dresden, Germany, vol. 4; p. 473 – 480.

17. Watmuff, J. H., Charters, W. W. S., Proctor, D., 1977. Solar and wind-induced external coefficients for solar collectors. Comples 2, 56.